

COLORIMETRIC SENSORS FOR FORMALDEHYDE DETECTION AND
ELECTROCHEMILUMINESCENT FOR PATHOGENS DETECTION



A Dissertation Submitted in Partial Fulfillment of the Requirements
for the Degree of Doctor of Philosophy in Chemistry

Department of Chemistry

FACULTY OF SCIENCE

Chulalongkorn University

Academic Year 2021

Copyright of Chulalongkorn University

เซ็นเซอร์เชิงสีสำหรับการตรวจวัดฟอร์มาลดีไฮด์และอิลีกโตรเคมีลูมิเนสเซนซ์สำหรับ
การตรวจวัดเชื้อโรค



วิทยานิพนธ์นี้เป็นส่วนหนึ่งของการศึกษาตามหลักสูตรปริญญาวิทยาศาสตรดุษฎีบัณฑิต
สาขาวิชาเคมี ภาควิชาเคมี
คณะวิทยาศาสตร์ จุฬาลงกรณ์มหาวิทยาลัย
ปีการศึกษา 2564
ลิขสิทธิ์ของจุฬาลงกรณ์มหาวิทยาลัย

อุมา พงษ์กิจเดชโชติ : เซ็นเซอร์เชิงสีสำหรับการตรวจวัดฟอร์มาลดีไฮด์และอิเล็กโตรเคมีลูมิเนสเซนซ์สำหรับการตรวจวัดเชื้อโรค. (COLORIMETRIC SENSORS FOR FORMALDEHYDE DETECTION AND ELECTROCHEMILUMINESCENT FOR PATHOGENS DETECTION) อ.ที่ปรึกษาหลัก : รศ. ดร.เฟื่องฟ้า อุ่นอบ

ในงานวิจัยนี้นำเสนอวิธีการตรวจวัดปริมาณฟอร์มาลดีไฮด์และวิธีการตรวจวัดปริมาณ *Cryptosporidium parvum* (*C. parvum*) ในตัวอย่างน้ำ สำหรับการตรวจวัดปริมาณฟอร์มาลดีไฮด์วิธีแรกอาศัยการเกิดอนุภาคระดับนาโนของเงินบนไฮดรอกซีแอฟาไทต์ผ่านปฏิกิริยาของ Tollens โดยไอออนเงินที่ถูกตรึงบนไฮดรอกซีแอฟาไทต์จะทำหน้าที่สกัดฟอร์มาลดีไฮด์ออกมาจากตัวอย่าง และเกิดปฏิกิริยา Tollens บนผิวของไฮดรอกซีแอฟาไทต์ หลังจากการเกิดปฏิกิริยาจะมีอนุภาคระดับนาโนของเงินเกิดขึ้นบนผิวของไฮดรอกซีแอฟาไทต์ ทำให้สีของวัสดุเปลี่ยนจากสีขาวเป็นสีเหลืองหรือสีน้ำตาล โดยความเข้มของสีขึ้นกับความเข้มข้นของฟอร์มาลดีไฮด์ ซึ่งปริมาณของฟอร์มาลดีไฮด์สามารถหาได้จากการหาความเข้มสีของไฮดรอกซีแอฟาไทต์ ภายใต้สภาวะที่เหมาะสม วิธีการนี้สามารถตรวจวัดปริมาณฟอร์มาลดีไฮด์ได้ในช่วงความเข้มข้น 15 – 200 ไมโครกรัมต่อลิตร และความเข้มข้นต่ำสุดที่สามารถวัดปริมาณฟอร์มาลดีไฮด์ได้อยู่ที่ 15 ไมโครกรัมต่อลิตร ทำการตรวจสอบความแม่นยำของวิธีวิเคราะห์โดยพิจารณาจากค่าการได้กลับของฟอร์มาลดีไฮด์ที่เติมลงไปตัวอย่างพบว่า มีค่าร้อยละการได้กลับในช่วง 86-111% โดยมีค่าเบี่ยงเบนมาตรฐานสัมพัทธ์น้อยกว่า 8% ในส่วนของการตรวจวัดปริมาณฟอร์มาลดีไฮด์อีกวิธี นำเสนอการตรวจวัดด้วยการใช้เจล agar-HPMC ตัดแปรผิวด้วย Schiff's reagent โดยฟอร์มาลดีไฮด์จะเกิดปฏิกิริยาของ Schiff ที่ผิวของเจลและแสดงสีม่วงบนเจล ซึ่งความเข้มของสีม่วงจะสัมพันธ์กับความเข้มข้นของฟอร์มาลดีไฮด์ในตัวอย่าง โดยความเข้มสีของเจลจะถูกวัดด้วยโปรแกรม Image-J จากการทดลองพบว่าภายใต้สภาวะที่เหมาะสม วิธีการนี้สามารถตรวจวัดปริมาณฟอร์มาลดีไฮด์ได้ในช่วงความเข้มข้น 2.00 – 10.00 มิลลิกรัมต่อลิตร และขีดจำกัดในการตรวจพบอยู่ที่ 1.49 มิลลิกรัมต่อลิตร ทำการตรวจสอบความแม่นยำของวิธีวิเคราะห์โดยพิจารณาจากค่าการได้กลับของฟอร์มาลดีไฮด์ที่เติมลงไปตัวอย่างพบว่า มีค่าร้อยละการได้กลับในช่วง 81-122% โดยมีค่าเบี่ยงเบนมาตรฐานสัมพัทธ์น้อยกว่า 16% ในส่วนสุดท้ายคือการตรวจวัดปริมาณ *C. parvum* ด้วยการใช้เทคนิค Sandwich hybridization assay ร่วมกับอิเล็กโตรเคมีลูมิเนสเซนซ์สำหรับการตรวจวัดปริมาณ *C. parvum* อาศัยการจับกันแบบจำเพาะเจาะจงระหว่าง capture DNA บนอนุภาคแม่เหล็กกับ *C. parvum* โดยการตรวจวัดด้วยอิเล็กโตรเคมีลูมิเนสเซนซ์ งานวิจัยนี้ได้ทำการขยายสัญญาณด้วยการใช้ไลโปโซมที่บรรจุ Tris(2,2'-bipyridine) ruthenium(II) ($Ru(bpy)_3^{2+}$) เพื่อเป็นตัวให้สัญญาณแก่เครื่องตรวจวัด ภายใต้สภาวะที่เหมาะสมพบว่า การใช้การตรวจวัดแบบขั้นตอนเดียวและสามขั้นตอน โดยใช้บัฟเฟอร์เป็นไฮบริดเชชันบัฟเฟอร์ ทำให้ได้สัญญาณในการตรวจวัด *C. parvum* สูงที่สุด โดยขีดจำกัดในการตรวจวัด *C. parvum* อยู่ที่ 0.039 และ 0.045 นาโนโมลต่อลิตรตามลำดับ ดังนั้นทั้งสองวิธีจึงถูกนำไปใช้ในการพัฒนาตรวจวัดปริมาณ *C. parvum* บนไมโครชิปต่อไป

CHULALONGKORN UNIVERSITY

สาขาวิชา เคมี
ปีการศึกษา 2564

ลายมือชื่อนิสิต
ลายมือชื่อ อ.ที่ปรึกษาหลัก

5972849623 : MAJOR CHEMISTRY

KEYWORD: formaldehyde, digital-image colorimetry, silver-doped hydroxyapatite, Schiff's reagent, agar gel, *Cryptosporidium parvum*, electrochemiluminescence, sandwich hybridization assay

Uma Pongkitdachoti : COLORIMETRIC SENSORS FOR FORMALDEHYDE DETECTION AND ELECTROCHEMILUMINESCENT FOR PATHOGENS DETECTION. Advisor: Assoc. Prof. FUANGFA UNOB, Ph.D.

In this work, two methods for the detection of formaldehyde and one assay for detection of *Cryptosporidium parvum* DNA (*C. parvum*) in water samples were developed. For the detection of formaldehyde, silver-doped hydroxyapatite (Ag-HAP) was used to extract formaldehyde from high volume samples and the Tollens' reaction occurred on the solid surface. After the reaction, silver nanoparticles were produced on the material resulting in the material color change from off-white to yellow or brown depending on the concentration of formaldehyde. By using the Ag-HAP, the detection of formaldehyde was achieved by measuring the color intensity. Under the optimized conditions, this method has a linear range of 15-200 $\mu\text{g L}^{-1}$ with the lowest concentration for detection of 15 $\mu\text{g L}^{-1}$. The recovery of formaldehyde in sample observed by the proposed method was 86-111% with relative standard deviation less than 8%. For another formaldehyde detection, the agar-HPMC gel modified with Schiff's reagent was used to detect formaldehyde in water samples. The detection of formaldehyde was based on Schiff's reaction on the gel surface. The magenta color product could be observed on the Schiff-gel after the contact with formaldehyde solution. The color intensity of the gel measured by Image-J software depended on the concentration of formaldehyde. Under the optimized conditions, the linear range was observed from 2.00-10.00 mg L^{-1} with the limit of detection was 1.49 mg L^{-1} . The recovery of formaldehyde in sample observed by the proposed method was 81-122% with the relative standard deviation less than 16%. For the detection of *C. parvum* DNA, the sandwich hybridization assay coupled with electrochemiluminescence measurement was designed and optimized. The detection of *C. parvum* DNA was based on the specific binding of capture DNA on magnetic beads and *C. parvum* DNA and the signal was amplified using liposomes containing Tris(2,2'-bipyridine) ruthenium(II) ($\text{Ru}(\text{bpy})_3^{2+}$) as reporter probe. Under the optimized conditions, the one-step, and three-step assay by using the hybridization buffer gave the high signal intensity with limit of detection of 0.039 nmol L^{-1} and 0.045 nmol L^{-1} , respectively. This assay was further investigated in the microfluidic chip.

Field of Study: Chemistry

Student's Signature

Academic Year: 2021

Advisor's Signature

ACKNOWLEDGEMENTS

First of all, I would like to express my sincere thanks to my dissertation advisor, Associate Professor Dr.Fuangfa Unob for her invaluable help and constant encouragement. I am grateful for her advice, not only for the research methodologies but also for many other things in my life. This dissertation would not have been completed without her support.

I would also like to thank Professor Dr.Antje Baeumner for providing me the opportunity to conduct collaborative research at Universität Regensburg. Thank all members of the workgroup Baeumner, especially: Florian Gerstl, Dr.Nongnoot Wongkaew, and Arne Behrent for their guidance during my stay in Regensburg. It has been my great pleasure working with them.

In addition, this dissertation would not have been accomplished without many precious and valuable advice and comments from my dissertation committee, Professor Dr.Vudhichai Parasuk, Assistant Professor Dr.Monpichar Srisa-Art, Associate Professor Dr.Boosayarat Tomapatanaget, and Associate Professor Dr.Atitaya Siripinyanond.

For all Environmental Analysis Research Unit members, I would like to acknowledge Associate Professor Dr.Wanlapa Aeungmaitrepirom, and Associate Professor Dr.Apichat Imyim for their valuable suggestions. Moreover, I would also like to thank all EARU members past and present for their friendships that made me feel good during the period of this research.

This research has been financially supported by the Development and Promotion of Science and Technology Talents Project (DPST).

Finally, I most gratefully acknowledge my family, especially my lovely parents for their love and unconditional support. Also, I would like to thank my best friend, Miss Nawaporn Khwanjaisakun, who has always believed in me. I would not be here without them!

Uma Pongkitdachoti

TABLE OF CONTENTS

	Page
ABSTRACT (THAI)	iii
ABSTRACT (ENGLISH)	iv
ACKNOWLEDGEMENTS	v
TABLE OF CONTENTS	vi
LIST OF TABLES	xi
LIST OF FIGURES.....	xiii
CHAPTER 1 INTRODUCTION	15
1.1 Rationales	15
1.2 Objectives of the research.....	17
1.3 Scope of the research	18
1.4 Theory and literature review of formaldehyde detection	18
1.4.1 Colorimetric detection of formaldehyde	18
1.4.2 Reaction for colorimetric detection of formaldehyde.....	20
a. Tollens' reaction.....	20
b. Schiff's reaction	21
1.4.3 Digital image based colorimetric detection of formaldehyde	22
1.4.4 Materials for formaldehyde detection.....	23
a. Hydroxyapatite	23
b. Agar	24
CHAPTER 2 COLORIMETRIC DETERMINATION OF FORMALDEHYDE USING SILVER-DOPED HYDROXYAPATITE	26

2.1 Experiments.....	27
2.1.1 Apparatus	27
2.1.2 Chemicals and reagent	27
2.1.3 Standardization of formaldehyde standard solution by the sulfite titration method.....	29
2.1.4 Determination of formaldehyde concentration in diluted standard solution by acetylacetone method.....	29
2.1.5 Synthesis of hydroxyapatite	30
2.1.6 Formaldehyde determination by silver-doped hydroxyapatite	30
a. Effect of silver ion concentration	31
b. Effect of sodium hydroxide concentration	31
c. Effect of contact time	31
d. Effect of sample volume	31
e. Selectivity study.....	31
2.1.7 The digital-image colorimetry procedure.....	32
2.1.8 Method validation.....	32
a. Calibration curve and linearity	33
b. Accuracy and precision in sample analysis.....	33
2.2 Results and discussion.....	34
2.2.1 Characterization of materials.....	34
a. X-ray diffraction (XRD)	34
b. Transmission electron microscopy (TEM).....	35
c. X-ray photoelectron spectroscopy (XPS).....	36
2.2.2 Optimization of parameters for formaldehyde detection	37

a.	Effect of silver ion concentration	37
b.	Effect of sodium hydroxide concentration	40
c.	Effect of contact time	42
d.	Effect of sample volume	43
2.2.3	Selectivity test.....	44
2.2.4	Method validation and sample analysis.....	47
CHAPTER 3 COLORIMETRIC DETERMINATION OF FORMALDEHYDE USING AGAR-HPMC COMPOSITE GEL MODIFIED WITH SCHIFF'S REAGENT		
3.1	Experiments.....	50
3.1.1	Apparatus	50
3.1.2	Chemicals and reagent	50
3.1.3	Preparation of Schiff-gel	51
3.1.4	Detection of formaldehyde	52
a.	Effect of Schiff's reagent concentrations.....	52
b.	Effect of contact time	53
3.1.5	The digital-image colorimetry procedure.....	53
3.1.6	Method performance and sample analysis.....	53
a.	Calibration curve and linearity	53
b.	Accuracy and precision in sample analysis.....	53
3.2	Results and discussion.....	54
3.2.1	Optimization of formaldehyde detection	54
a.	Effect of Schiff's reagent concentration	54
b.	Effect of contact time	56
3.2.2	Method performance and sample analysis	58

a.	Calibration curve and linearity	59
b.	Water samples analysis.....	59
3.3	Comparison of method performance.....	61
CHAPTER 4 ELECTROCHEMILUMINESCENT DETECTION OF PATHOGENS ON MICROFLUIDIC DEVICE		64
4.1	Introduction.....	64
4.1.1	Rationales.....	64
4.1.2	Theory of this work.....	66
a.	Electrochemiluminescence (ECL).....	66
b.	Sandwich hybridization assay	67
c.	Liposomes	67
4.1.3	Objective of this work.....	68
4.2	Experiments.....	68
4.2.1	Apparatus	68
4.2.2	Chemicals and reagent	68
4.2.3	Assay with magnetic beads.....	72
a.	Preliminary test	72
b.	The amount of Ru(bpy) ₃ ²⁺ -liposomes.....	74
c.	The amount of magnetic beads	74
d.	The number of assay steps.....	75
4.2.4	ECL measurement.....	75
4.2.5	Fluorescence measurement.....	75
4.3	Results and discussions.....	76
4.3.1	Preliminary test.....	76

4.3.2 The amounts of liposomes.....	77
4.3.3 The amount of magnetic beads.....	78
4.3.4 The number of assay steps	79
CHAPTER 5 CONCLUSION	82
REFERENCES.....	84
VITA	93



LIST OF TABLES

	Page
Table 2.1 List of analytical apparatus.....	27
Table 2.2 List of chemicals.....	27
Table 2.3 The effect of silver ion concentration for HAP modification on the color of AgNPs-HAP used in formaldehyde detection.....	38
Table 2.4 The effect of sodium hydroxide concentration on the color of AgNPs-HAP used in formaldehyde detection.....	41
Table 2.5 The effect of contact time on the color of AgNPs-HAP used in formaldehyde detection.....	42
Table 2.6 The color of Ag-HAP observed with various of sample volume.....	44
Table 2.7 Results from water sample analysis using the silver-doped hydroxyapatite method and the HPLC method.....	48
Table 3.1 List of analytical apparatus.....	50
Table 3.2 List of chemicals.....	50
Table 3.3 The effect of Schiff's reagent concentrations on the Schiff-gel color observed in the formaldehyde detection.....	55
Table 3.4 The effect of contact time on the color of Schiff-gel prepared with 2.00 and 2.50 mmol L ⁻¹ Schiff's reagent observed in formaldehyde detection.....	57
Table 3.5 Analytical results and recoveries of formaldehyde determination in water samples by the proposed method.....	60
Table 3.6 Comparison of colorimetric methods for formaldehyde detection.....	61
Table 4.1 List of analytical apparatus.....	68
Table 4.2 List of chemicals and materials.....	68
Table 4.3 The sequences of all C. parvum probes for this work.....	70



จุฬาลงกรณ์มหาวิทยาลัย
CHULALONGKORN UNIVERSITY

LIST OF FIGURES

	Page
Figure 1.1 The reaction mechanism between Schiff's reagent and aldehyde	22
Figure 1.2 Crystal planes of hydroxyapatite	24
Figure 1.3 The structure of agarose	25
Figure 2.1 Schematic of the developed method for formaldehyde detection.	26
Figure 2.2 XRD pattern of the hydroxyapatite prepared by co-precipitation method compared to JCPDS card 9-0432 (below)	35
Figure 2.3 TEM images of hydroxyapatite (A) before formaldehyde detection and (B) after the detection of $50 \mu\text{g L}^{-1}$ formaldehyde. Red arrows highlight silver nanoparticles on the surface.	36
Figure 2.4 The XPS spectra of AgNPs-HAP obtained after the detection of $70 \mu\text{g L}^{-1}$ formaldehyde and corresponding deconvoluted peaks of Ag (3d).	37
Figure 2.5 The Δ intensity of materials color observed in the detection of formaldehyde by Ag-HAP prepared by using various silver ion concentrations.	39
Figure 2.6 Effect of silver ion concentrations on the efficiency of silver ions adsorption on hydroxyapatite	40
Figure 2.7 The Δ intensity of materials color observed in the analysis of formaldehyde solutions containing different sodium hydroxide concentrations.	41
Figure 2.8 The Δ intensity of Ag-HAP color observed by using different contact times for detection of formaldehyde	43
Figure 2.9 The Δ intensity of Ag-HAP color observed by using different sample volumes	44
Figure 2.10 The Δ intensity of Ag-HAP color observed in the detection of (A) formaldehyde and various compounds (B) formaldehyde in the absence (only formaldehyde) and in the presence of various compounds.	45

Figure 2.11 The calibration curve for formaldehyde determination and the observed materials color after formaldehyde detection.....	47
Figure 3.1 The analytical procedure for formaldehyde detection by Schiff-gel.....	52
Figure 3.2 The Δ intensity of agar-HPMC color after detection of formaldehyde with various of Schiff's reagent on Schiff-gel.....	56
Figure 3.3 The Δ intensity of Schiff-gel prepared with (A) 2.00 mmol L ⁻¹ Schiff's reagent and (B) 2.50 mmol L ⁻¹ Schiff's reagent obtained from formaldehyde detection using different contact times.....	58
Figure 3.4 The calibration curve for formaldehyde determination and the observed color of Schiff-gel after formaldehyde detection.....	59
Figure 4.1 Schematic of the developed assay for <i>C. parvum</i> DNA detection by ECL. .	66
Figure 4.2 One possible mechanism of Ru(bpy) ₃ ²⁺ -ECL.....	67
Figure 4.3 The procedure of preliminary test (A) assay A - two-step/binding cDNA in centrifuge tube, (B) assay B - three-step/binding cDNA in centrifuge tube, (C) assay C - three-step/binding cDNA in well plate.....	74
Figure 4.4 Steps in performing the assay: assay A - two-step/binding cDNA in centrifuge tube, assay B - three-step/binding cDNA in centrifuge tube, assay C - three-step/binding cDNA in well plate.....	77
Figure 4.5 Effect of the liposomes amount in the detection of tDNA (100 nmol L ⁻¹) in the three-step assay compared to blank (n=4).....	78
Figure 4.6 Effect of magnetic beads amount (50 and 100 μ g) and the mole ratio of streptavidin on magnetic beads and cDNA on the detection of 100 nmol L ⁻¹ tDNA in three-step assay (n=4).	79
Figure 4.7 (A) the procedure for all assays, the dose-response curve obtained by (B) ECL measurement and (C) fluorescence measurement (n=4).	81

CHAPTER 1

INTRODUCTION

1.1 Rationales

The contamination of toxic chemicals or pathogen in water is an important issue because it directly affects human health. Pathogen is defined as a microbial that can cause consumer illness and even low concentrations of pathogen in water can cause the early stage of infection in humans [1]. In addition, formaldehyde is a chemical widely used for preserving biological specimens [2] and preventing parasitic infection in fishpond [3]. It could also be found as a byproduct in water treatment process such as ozonation or chlorination [4, 5]. Due to health concerns, the World Health Organization (WHO) established a regulation on the level of formaldehyde in drinking water. This level should not exceed $100 \mu\text{g L}^{-1}$ or $3.3 \mu\text{mol L}^{-1}$ [6]. Human may expose to formaldehyde through inhalation, ingestion, contact with skin or eyes. Exposure to high levels of formaldehyde can cause acute irritation to skin, respiratory system, and digestive system. Long-term exposure to low levels of formaldehyde can cause accumulation in the human body and may lead to cancer [7]. Therefore, monitoring pathogen and formaldehyde in water runoff and resources are necessary.

There are many reported methods for formaldehyde detection using analytical instruments including high performance liquid chromatography (HPLC) [8, 9], gas chromatography (GC) [10], UV-Vis spectrophotometry, spectrofluorometry [11-17]. HPLC and GC are the commonly used techniques for trace formaldehyde detection. Even though these methods are selective and sensitive for formaldehyde detection, each method still requires high-cost equipment and well-trained users. The use of colorimetric probe coupled with a simple analytical instrument such as UV-Vis spectrometer or spectrofluorometer became an interesting alternative for formaldehyde detection. Many colorimetric probes were developed using various chromophores including resorcinol functionalized AuNPs [11], dyes [12, 13], and fluorescent compounds [14, 15]. Nevertheless, the preparation of these probes was

complicated. By using simpler colorimetric reagents, the Tollens' reaction and Schiff's reaction have been used to detect formaldehyde in samples.

Tollens' reaction requires a simple reagent mixture including silver ions and base. To improve the sensitivity for trace formaldehyde detection, the reagents was modified with nanoparticles [16, 17]. Furthermore, Schiff's reaction is based on the reaction between aldehyde and Schiff's reagent (product of rosaniline hydrochloride reacted with sodium sulfite) [18]. The product of this reaction gives the magenta color. Although, these methods have high sensitivity for formaldehyde detection, they still required a UV-Vis spectrophotometer. The development of sensitive analytical methods for formaldehyde detection without the requirement of an analytical instrument is challenging. Digital-image colorimetry has gained popularity as an alternative for instrument-free colorimetric detection.

Digital-image colorimetry for formaldehyde detection using Schiff's reagent was proposed [19]. The sample color was observed after releasing the Schiff's reagents into the sample solution. Despite the simplicity, the method was not sensitive enough for low-level detection of formaldehyde. The sample matrix and color could strongly interfere the colorimetric detection. The separation of formaldehyde from a sample by extraction onto a separated phase will reduce the sample matrix and pre-concentrate the analyte for the detection. As for example, head space single drop-microextraction coupled with a gold nanoprism/Tollens' reagent complex was applied for the detection of formaldehyde with digital-image colorimetry [20]. The vapor of formaldehyde was evaporated from the sample to the single drop containing reagent. Even though the matrix effect was overcome and trace level analysis could be achieved, it might be difficult to control the evaporation of formaldehyde. To solve this problem, extraction of formaldehyde on to solid materials is an alternative. Herein, two methods for digital-image based colorimetric detection of formaldehyde were developed based on i) Tollens' reaction on silver-doped hydroxyapatite and ii) Schiff's reaction on agar-HPMC gel modified with Schiff's reagent (Schiff-gel).

For the first method, hydroxyapatite (HAP) was chosen as a material for bearing Tollens' reagent for formaldehyde detection. Hydroxyapatite ($\text{Ca}_{10}(\text{PO}_4)_6(\text{OH})_2$)

is a biomaterial that has unique adsorption properties such as high surface area to volume ratio and ion exchange property [21]. In this proposed method, hydroxyapatite was modified with silver ions (Ag-HAP) through ion-exchange with calcium ions and used to detect formaldehyde in the water samples. On the surface of Ag-HAP, the silver ions were reduced to silver nanoparticles in the presence of formaldehyde in solution under basic condition. The colorimetric detection was achieved by observing the material color change. The color intensity of silver nanoparticles on the material depended on the formaldehyde concentration.

In the second method, the composite gel made from agar and hydroxypropyl methylcellulose (HPMC) was chosen as a detection platform after modifying with Schiff's reagent. These materials were hydrophilic, non-toxic, and low cost. The components could interact well with each other through intermolecular force [22] and hence, the homogenous composite gel (Agar-HPMC gel) could be obtained. The Agar-HPMC composite gel was modified with Schiff's reagent (Schiff-gel) and used to detect formaldehyde in water samples. Formaldehyde in samples reacted with the Schiff's reagent on the composite gel, yielding a magenta product on the gel. The gel color changed from pale yellow to magenta that could be observed by naked eyes and the color intensity is obtained by measuring the color intensity by Image-J program.

For detection of pathogen contaminated in water, highly sensitive and specific detection methods are required to monitor these pathogens. In this work, *Cryptosporidium parvum* (*C. parvum*) was chosen as a model pathogen. A new assay for *C. parvum* detection based on electrochemiluminescence was developed (see the detail in the Chapter IV).

1.2 Objectives of the research

The objectives of the research are listed below,

- To develop a silver-doped hydroxyapatite method for detection of formaldehyde in water samples based on Tollens' reaction.
- To develop a gel platform from Agar-HPMC gel modified with Schiff's reagent for detection of formaldehyde in water samples.

- To develop an electrochemiluminescence assay for detection of pathogens in water samples.

1.3 Scope of the research

In this work, two methods for formaldehyde detection were developed, including a method based on Tollens' reaction on hydroxyapatite and Schiff's reaction on Agar-HPMC composite gel. Hydroxyapatite was prepared by the co-precipitation method and modified with silver ions as the reagent for Tollens' reaction. For the Agar-HPMC composite gel method, Agar-HPMC was prepared and modified with Schiff's reagent. The detection of formaldehyde occurred via the aldimine condensation reaction. The effect of parameters affecting the detection of formaldehyde on each material was investigated and optimized. The performance of the proposed methods was evaluated by using the optimized method to detect formaldehyde in water samples. For the detection of pathogen, *Cryptosporidium parvum* (*C. parvum*) was chosen as a pathogen model. An electrochemiluminescence (ECL) assay was developed. The effect of parameters affecting the detection of *C. parvum* on the assay was investigated.

1.4 Theory and literature review of formaldehyde detection

1.4.1 Colorimetric detection of formaldehyde

Colorimetric analysis is a commonly used method to determine the analyte concentration via observing color changes of the solution or material. Many researchers have reported the application of various colorimetric probes for formaldehyde determination. In 2019, Martinez-Aquino and co-workers [11] applied gold nanoparticles modified with resorcinol as a colorimetric probe for detection of formaldehyde. The aggregation of gold nanoparticles was induced by the crosslink reaction of resorcinol on the particles by formaldehyde in solution. The interparticle-crosslink aggregation resulted in a change in the surface plasmon resonance absorption, and thus, the color of solution changed from red to purple. The detection limit of this method was as low as 0.5 mg L^{-1} and this probe was used to detect formaldehyde in composite wood board.

In the same year, Wei and coworkers [12] reported the use of heptamethinecyanine derivative as a two-step responsive colorimetric probe for formaldehyde detection. Formaldehyde reacted with primary amine on this probe structure, yielding a new structure which possessed a higher pKa value compared to the starting molecule. This product showed green color when protonated (pH 3-6). This probe could detect formaldehyde in a short time (30 s). Under weakly acidic conditions, the solution color was changed from blue to green in the presence of formaldehyde. The proposed probe provided a detection limit of 0.098 mg L^{-1} formaldehyde, and it was suitable for the detection of formaldehyde in acidic solution.

In 2020, Gao and coworkers [13] proposed a method for formaldehyde detection based on the decolorization phenomenon of ortho-aniline aromatic azo dyes. The dyes were synthesized and modified on silk fibroin. When exposed to formaldehyde, these dyes reacted with the formaldehyde via Mannich reaction, disrupting the conjugation system of the dye and further resulting in the color fading. The detection limit of this work was 0.123 mg L^{-1} .

Moreover, some researchers reported the use of fluorescence probes for the determination of formaldehyde. In 2016, Aksornneam and coworkers [14] demonstrated the use of polyvinyl alcohol (PVA) film containing 5-aminofluorescein for detection of formaldehyde. The principle of detection was based on the reaction between formaldehyde and primary amine of 5-aminofluorescein to produce an imine functional group. After the reaction, strong yellow-green fluorescence was observed, and the fluorescence emission was measured by a spectrofluorometer. This film allowed the detection of formaldehyde as low as $3.820 \text{ } \mu\text{g L}^{-1}$ and was used to detect formaldehyde in vegetable and seafood.

In 2018, Li and coworkers [15] prepared hydrazino-naphthalimide grafted chitosan as a fluorescence probe for formaldehyde detection. The response of this probe depended on the specific reaction between formaldehyde and hydrazine group to trigger a turn-on fluorescence signal. The detection limit of the method was 0.05 mg L^{-1} and the proposed probe was used to detect formaldehyde in food and water samples.

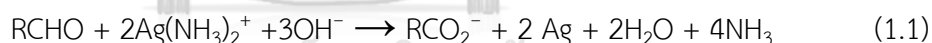
Although the detection of formaldehyde using these colorimetric probes is selective and sensitive, the preparation of the probes was complicated. Commonly used reactions for colorimetric detection of formaldehyde including Tollens' reaction and Schiff's reaction are still drawing interest due to their simplicity. By applying these reactions on different detection platforms, new methods for sensitive formaldehyde detection have been proposed.

1.4.2 Reaction for colorimetric detection of formaldehyde

The well-known reactions for testing formaldehyde such as Tollens' reaction [23], Schiff's reaction [18], or reaction with acetylacetone reagent [24] have been applied in the detection of formaldehyde. In this work, we focus on the Tollens' reaction and Schiff's reaction.

a. Tollens' reaction

Tollens' reaction is used to distinguish aldehyde from ketone functional group. In this reaction, aldehyde acts as a reducing agent. It reacts with Tollen's reagent ($[\text{Ag}(\text{NH}_3)_2]\text{OH}$) under a basic condition to produce elemental silver as shown in equation 1.1 [23]:



Several researchers presented colorimetric methods for formaldehyde detection based on the reducing properties of formaldehyde. These proposed methods used Tollens' reagent coupled with nanoparticles for improving the detection sensitivity. In 2014, Zeng and coworkers [16] used gold nanoparticles coupled with Tollen's reagent for detecting formaldehyde in solution. In this study, formaldehyde reduced silver ions to silver nanoparticles that further deposited on gold nanoparticles to form silver shell. The thickness of silver shell on gold nanoparticles depended on the formaldehyde concentrations in the sample. The color of solution changed from pink to deep yellow when the formaldehyde concentration increased. The absorbance was measured by a UV-vis

spectrophotometer. This method was used to detect formaldehyde in aqueous solution with a detection limit of $1.5 \mu\text{g L}^{-1}$.

In 2018, Chaiendoo and coworkers [17] developed a method for formaldehyde detection using silver nanoclusters modified Tollen's reagent. Silver ions in Tollen's reagent was reduced by formaldehyde and deposited onto the nanocluster. The results showed a color change caused by the change in the particle size from silver nanoclusters to silver nanoparticles. This method was applied to detect formaldehyde in squid and ground chicken samples. The absorbance of solution was measured by a UV-vis spectrophotometer. This method could detect formaldehyde with a detection limit of 0.84 mg L^{-1} .

In 2020, Qi and coworkers [20] reported a method for detection of trace formaldehyde in sample solution by head space single drop-microextraction coupled with a gold nanoprism/Tollens' reagent complex (Au-np/TR). In this method, a drop containing reagent complex was hung on the lid of sample tube. Then, formaldehyde gas was evaporated from sample solution to react with silver ions in Au-np/TR inside the drop. The color of reagent drop was observed by taking photograph, and their color intensity was analyzed using the EKcolorpicker software in blue mode. This method provided the detection of formaldehyde in a range of $0.003 - 3 \text{ mg L}^{-1}$ with a detection limit of 0.0009 mg L^{-1} .

b. Schiff's reaction

Schiff's reaction is the general chemical reaction for aldehyde detection first introduced by Hugo Schiff [18]. The Schiff's reagent is a dye product from the reaction between rosaniline hydrochloride and sodium sulfite. The Schiff's reagent is stable and has yellow color in acidic solution. After testing with aldehyde, the color changes from yellow to magenta depending on the aldehyde concentration [18]. The structure of Schiff's reagent prepared by the reaction between rosaniline hydrochloride and sodium sulfite in an acid condition is shown Figure 1.1. The reaction of the reagent with aldehyde is also shown.

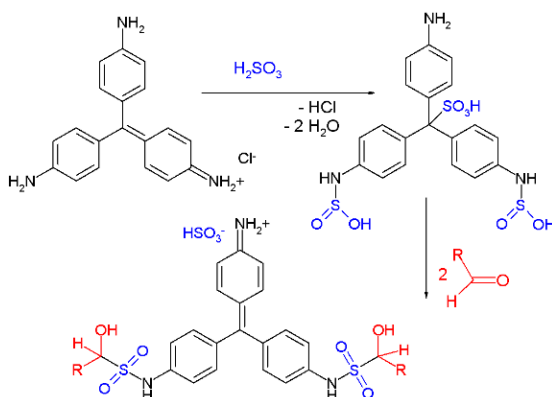


Figure 1.1 The reaction mechanism between Schiff's reagent and aldehyde [18].

Some researchers presented colorimetric methods for formaldehyde detection using Schiff's reagent. In 2007, Maruo and coworker [25] prepared a porous glass impregnated with Schiff's reagent for detection of formaldehyde in the air. The color of sensor changed from yellow to purple after being exposed to formaldehyde gas and the absorbance of the sensor was measured by a spectrometer. The result showed that this sensor could detect formaldehyde gas in the range of $10 \mu\text{g L}^{-1}$ to 20mg L^{-1} after 1 hr exposure to formaldehyde gas.

In 2021, Silva and coworker [19] proposed a method for detection of formaldehyde in milk samples based on Schiff's reaction. After protein precipitation, the sample solution was mixed with Schiff's reagent in Eppendorf tubes. After 35 min of reaction time, the photo of sample solution was taken by a smartphone and the color intensity was measured in RGB mode. The detection limit of $120 \mu\text{g L}^{-1}$ was reported.

From the literature review, Tollens' reagent and Schiff's reagent have been applied for low-level formaldehyde detection. These methods have high sensitivity and selectivity. However, most of these methods still required analytical equipment for the detection.

1.4.3 Digital image based colorimetric detection of formaldehyde

Some researchers presented alternative methods for trace formaldehyde detection using the digital-image colorimetry such as the methods proposed from Qi

and co-workers [20], and Silva and coworker [19] as described previously. Moreover, the use of smartphone for detection of formaldehyde was presented by Wongniramaikul and coworkers in 2018 [26]. They presented the method for detection of formaldehyde via Hantzsch reaction on film. They entrapped acetylacetone in a biodegradable film casted on the lid of a centrifuge tube. In the detection step, the film was dissolved when mixed with aqueous samples. The reagent was released into the sample solution to react with formaldehyde. The solution color changed to yellow depending on the concentration of formaldehyde. Then, the photo of solution was taken by a smartphone, and the color intensity was measured using in-house RGB analysis program. The detection limit of 0.7 mg L^{-1} was reported.

From the literature review described previously, many researchers attempted to develop instrument-free methods for formaldehyde detection using digital image-based colorimetry. Most methods still suffered from poor sensitivity. In this research, we focused on the development of an instrument-free method for trace formaldehyde detection based on Tollens' reaction or Schiff's reaction on a solid surface.

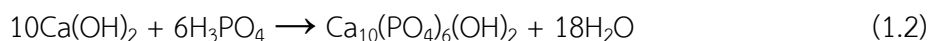
1.4.4 Materials for formaldehyde detection

For improving the sensitivity of formaldehyde detection, the use of solid phase extraction is an alternative. The benefit of solid phase extraction is that it allows the analysis of high-volume samples. In this work, we are interested in using hydroxyapatite and agar as they are hydrophilic, non-toxic, and low cost.

a. Hydroxyapatite

Hydroxyapatite ($\text{Ca}_{10}(\text{PO}_4)_6(\text{H}_2\text{O})_2$) is a biomaterial that consists of calcium and phosphate at a ratio of 1.67 [27]. It has found applications in various fields including biomedical, catalysis, pharmaceutical, and water treatment process. For the synthesis of hydroxyapatite, it can be synthesized using different techniques including dry, wet, and high-temperature methods. The co-precipitation method is the one of the wet processes that is commonly used to synthesize hydroxyapatite. In this method,

calcium solution and phosphate solution are mixed under a basic condition and the hydroxyapatite was formed following the equation 1.2 [28].



The hydroxyapatite is stable at the room temperature and in solution pH between 4 -12. It has a hexagonal crystalline structure with two major crystal planes including a plane and c plane as shown in Figure 1.2. In a plane, it is rich in calcium ions while c plane contains more of phosphate and hydroxide ions. Therefore, a plane and c plane show positive charge and negative charge, respectively. Due to the structure of hydroxyapatite, the calcium ions can be replaced with other cation ions (e.g. silver ions, magnesium ions, sodium ions, and potassium ions) through the ion exchange mechanism [27]. In this study, hydroxyapatite was used and modified with silver ions on the surface for further application in formaldehyde detection based on Tollens' reaction.

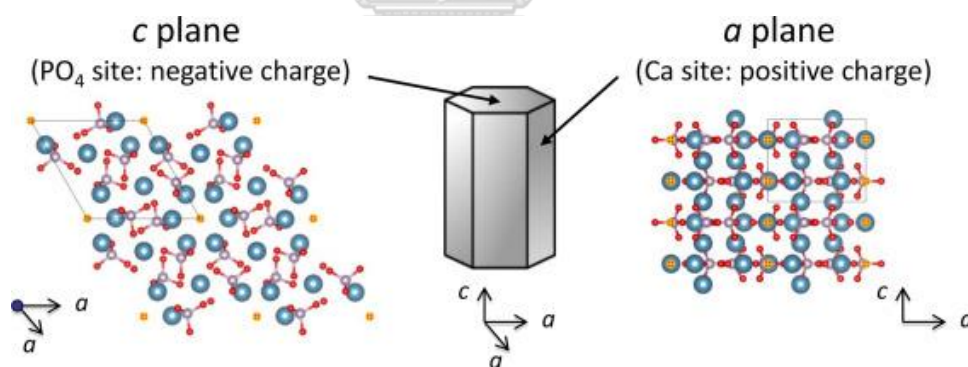


Figure 1.2 Crystal planes of hydroxyapatite[27].

b. Agar

Agar powder is a natural polymer obtained from the marine algae. Agar consists of two polysaccharides including agarose (linear chain) and agaropectin. 70% of agar is agarose, it is a linear polymer of D-galactose and 3,6-anhydro-L-galactopyranose. The structure of agarose is shown in Figure 1.3.

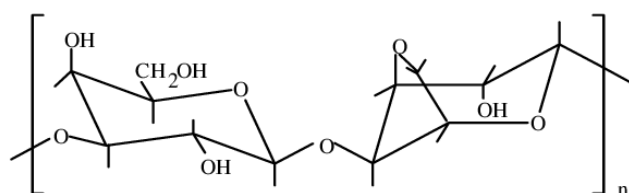


Figure 1.3 The structure of agarose[29].

Agar solidifies at about 32 – 40 °C and melts at 85 °C [30]. This property gives agar the advantages of easy gel formation and supporting material preparation. However, agar solution for supporting material preparation is viscous and turned to gel before setting in the mold. To solve this problem, hydroxypropyl methylcellulose (HPMC) can be added to agar solution to reduce the viscosity. In this composite, HPMC acts as a disintegration regulator [29].

In this work, HAP and Agar-HPMC composite gel were used as material for formaldehyde detection based on Tollens' reaction and Schiff's reaction, respectively.

CHAPTER 2

COLORIMETRIC DETERMINATION OF FORMALDEHYDE USING SILVER-DOPED HYDROXYAPATITE

In this part, the colorimetric method is proposed for the determination of formaldehyde in water samples by silver-doped hydroxyapatite. The silver-doped hydroxyapatite was prepared by modification of silver ions on the hydroxyapatite via ion-exchange with calcium ions. On the surface of Ag-HAP, the silver ions were reduced to silver nanoparticles in the presence of formaldehyde in solution under a basic condition. The colorimetric detection was achieved by observing the material color change. The color intensity of silver nanoparticles on the material depended on the formaldehyde concentration. The change of material color could be observed by naked eyes and the color intensity was measured by Image-J software. By using Ag-HAP in the detection, large volume of sample could be applied in the extraction and detection, enhancing the detection sensitivity. A schematic of the proposed method is shown in Figure 2.1. The reaction between formaldehyde and Tollens' reagent was occurred following the equation 1.1.

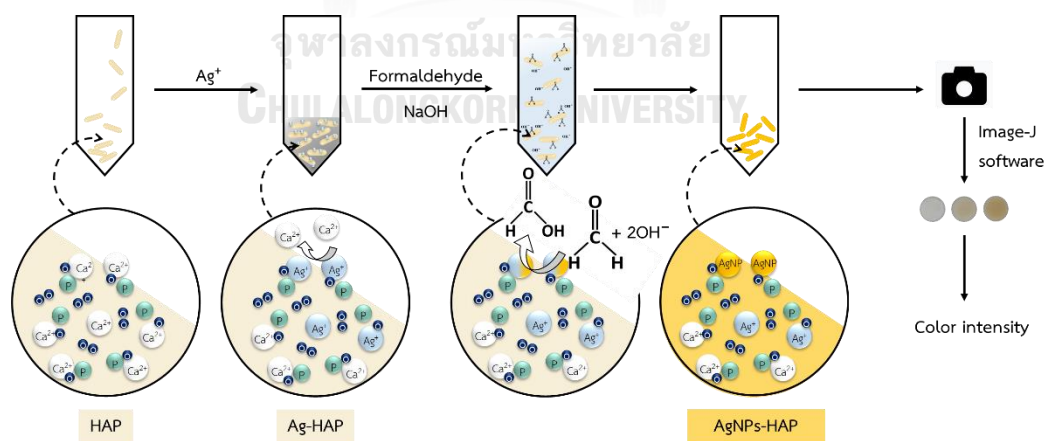


Figure 2.1 Schematic of the developed method for formaldehyde detection.

2.1 Experiments

2.1.1 Apparatus

Table 2.1 List of analytical apparatus.

Apparatus	Manufacturing/Models
Centrifuge	Hettich Zentrifugen/D-78532 Tuttlingen
High-performance liquid chromatograph (HPLC)	Agilent/1260 Infinity II Quaternary System
Inductively coupled plasma-optical emission spectrometer (ICP-OES)	Thermo/iCAP 6000 Series
Oven	Memmert/UM 500
pH meter	Mettler TOLEDO/Seven compact model
Smartphone	Samsung galaxy A5 (2016)/SM-A510FD
Transmission electron microscope (TEM)	Hitachi/S-4800
UV-visible spectrophotometer	Agilent/Hewlett Packard/HP 8453
X-ray photoelectron spectrometer (XPS)	Kratos/Axis ultra DLD
X-ray diffraction spectrometer (XRD)	Bruker AXS/Diffractometer D8

2.1.2 Chemicals and reagent

Table 2.2 List of chemicals.

Chemicals	Supplies
Acetic acid (CH ₃ COOH)	Merck
Acetylacetone	Carlo Erba
Ammonium acetate	J.T. Baker
Ammonium hydroxide (NH ₄ OH)	Carlo Erba
Calcium nitrate (Ca(NO ₃) ₂)	Thermo Fisher Scientific
Formaldehyde (40% w/v)	Carlo Erba
Hydrochloric acid (HCl)	Merck
Phosphoric acid (H ₃ PO ₄)	Carlo Erba

Table 2.2 List of chemicals. (Cont.)

Chemicals	Supplies
Silver nitrate (AgNO ₃)	Merck
Sodium bicarbonate (NaHCO ₃)	Merck
Sodium hydroxide (NaOH)	Merck
Sodium sulfite (Na ₂ SO ₃)	Merck

All chemicals were of analytical grade and used without further purification. The reagents were prepared using milliQ water as described as followed.

Formaldehyde solution

A 1000 mg L⁻¹ formaldehyde standard solution was prepared and used as a stock solution by diluting 40% (w/v) formaldehyde solution with milliQ water. The concentration of stock formaldehyde solution was determined by titration method [31-33]. A 1000 µg L⁻¹ formaldehyde standard solution was prepared by diluting the stock formaldehyde solution with milliQ water and the exact concentration of the prepared solution was determined by the acetylacetone method using UV-Vis spectrophotometer [24, 34]. This solution was further used to prepare working standard solutions in the concentration range of 15-200 µg L⁻¹.

Acetylacetone reagent

Acetylacetone reagent was prepared by mixing 7.5 g of ammonium acetate, 150 µL of acetic acid (100% v/v), and 100 µL of acetylacetone (99.5% v/v) in 50.00 mL milliQ water. This acetylacetone reagent was used for determining formaldehyde concentration using a UV-Visible spectrometer.

Silver ions solutions

A 0.01 mol L⁻¹ stock silver ions solution was prepared by dissolving 16.99 mg of silver nitrate (AgNO₃) in 10 mL of milliQ water. The stock solution was further used to modify hydroxyapatite. The exact concentration of stock silver ions solution was determined by ICP-OES before use.

2.1.3 Standardization of formaldehyde standard solution by the sulfite titration method

A solution of 1.13 mol L^{-1} sodium sulfite was prepared and used for the standardization of formaldehyde solution. The pH value of 10.00 mL of sodium sulfite solution was measured as initial pH before mixing with 10.00 mL of 1000 mg L^{-1} of formaldehyde solution. The pH of the mixture was measured. Then, HCl solution (0.1 mol L^{-1}) as a titrant was added into the solution to bring the mixture pH back to the initial value. The volumes of HCl solution added were recorded [31-33]. The reaction of formaldehyde with sodium sulfite is shown in equation 2.1.



The concentration of formaldehyde stock solution was calculated using equation (2.2). The stock solution of formaldehyde must be standardized before use. The HCl solution was also standardized before use using sodium bicarbonate solution and methyl red as indicator.

$$\text{Formaldehyde} \left(\frac{\text{mg}}{\text{mL}} \right) = \frac{(V_{\text{HCl}})(C_{\text{HCl}})(30.03)}{(V_{\text{formaldehyde}})} \quad (2.2)$$

30.03 is molar mass of formaldehyde

C_{HCl} is the concentration of HCl (mol L^{-1})

V_{HCl} is the volume of HCl (mL) used for titration

$V_{\text{formaldehyde}}$ is the volume of formaldehyde stock solution (mL)

2.1.4 Determination of formaldehyde concentration in diluted standard solution by acetylacetone method

The acetylacetone reagent (0.02 mol L^{-1} , 5.00 mL) was mixed with formaldehyde standard solutions, stirred for 30 min at $45 \text{ }^\circ\text{C}$, and left at room temperature for another 30 min. After that, the solution was analyzed by a UV-Vis spectrophotometer and the absorbance at 412 nm was recorded. To determine the

formaldehyde concentration, an external standard calibration curve was constructed in a concentration range from 0.20 – 1.20 mg L⁻¹.

2.1.5 Synthesis of hydroxyapatite

Hydroxyapatite was synthesized via co-precipitation between Ca(NO₃)₂ and H₃PO₄ solution at a Ca/P ratio of 1.67 [21]. The pH of the mixture was adjusted to 11 by ammonia solution (25% v/v). After that, the mixture was stirred for 2 hr. The obtained solid was filtered, washed with milliQ water to remove the residual base, and dried overnight in an oven at 120°C. The obtained material was characterized by X-ray diffraction (XRD) and transmission electron microscopy (TEM).

2.1.6 Formaldehyde determination by silver-doped hydroxyapatite

The analytical procedure for detection of formaldehyde by silver-doped hydroxyapatite is presented in Figure 2.1. 40 mg of hydroxyapatite was modified with silver ions by stirring the material with silver nitrate solution (1.00 mL) for 2 min. The solid was separated by centrifugation and immediately mixed with formaldehyde solution and 0.150 mL of sodium hydroxide. Then, the mixture was stirred for a specific period before the solid separation. The solid was further spread onto a filter paper No. 1 and put in a studio box with controlled brightness (see detail in 2.1.7). Photos of the resulting material were taken with controlled distance between the material and smartphone (15 cm). The image was subjected to Image-J software to determine the color intensity in RGB mode, and the blue values (I) were collected. The results were presented in term of Δ intensity (ΔI), calculated by equation 2.3.

$$\Delta \text{intensity} = I_{\text{blank}} - I_{\text{AgNPs-HAP}} \quad (2.3)$$

I_{blank} and $I_{\text{AgNPs-HAP}}$ are the color intensities of the material observed in the absence of formaldehyde (blank) and that of the material used in formaldehyde detection (AgNPs-HAP).

a. Effect of silver ion concentration

Silver ions solutions ($50 - 100 \text{ mg L}^{-1}$) were prepared by diluting a 0.1 mol L^{-1} silver ions stock solution with milliQ water. Then, 1.00 mL of each silver ions solution was mixed with 40 mg of hydroxyapatite for 2 min under continuous stirring. The solid was separated by centrifugation. The Ag-HAP material obtained was subsequently used to detect formaldehyde in standard solutions ($10 - 150 \text{ } \mu\text{g L}^{-1}$). After solid separation, the photo of the obtained solid was captured by a smartphone and the color intensity of material was measured using Image-J software. To determine the amount of silver ions adsorbed, the concentration of silver ion in the solution before and after the hydroxyapatite modification was determined by ICP-OES.

b. Effect of sodium hydroxide concentration

To study the effect of sodium hydroxide on formaldehyde detection by Ag-HAP, the concentration of sodium hydroxide in formaldehyde solution was varied in the range of $0.10 - 0.25 \text{ mol L}^{-1}$. Formaldehyde concentration was in a range of $10 - 100 \text{ } \mu\text{g L}^{-1}$. The Ag-HAP was prepared by using 100 mg L^{-1} silver ions solution to modify hydroxyapatite. The suitable sodium hydroxide concentration for this reaction was selected for further experiment.

c. Effect of contact time

The effect of contact time on formaldehyde detection was examined in the range of $30 - 90 \text{ min}$. The solutions containing formaldehyde in a concentration range of $10 - 100 \text{ } \mu\text{g L}^{-1}$ and 0.15 mol L^{-1} sodium hydroxide were used for this study.

d. Effect of sample volume

The effect of sample volume was investigated in the range of $3.00 - 10.00 \text{ mL}$. The detection of formaldehyde standard solution ($10 - 50 \text{ } \mu\text{g L}^{-1}$) containing 0.15 mol L^{-1} sodium hydroxide was performed with a contact time of 30 min .

e. Selectivity study

The selectivity of the proposed method was evaluated by applying the method to analyze formaldehyde standard solution in the absence and in the presence of different compounds (i.e. acetone, ethanol, formic acid, acetic acid, and

other aldehyde) or salt commonly found in water (i.e. NaCl, NaH₂PO₄, and Na₂SO₄) as binary mixtures. The concentration of formaldehyde was 1.0 μmol L⁻¹, while 50 μmol L⁻¹ of different organic compounds, or 10 mmol L⁻¹ of salt were present in the binary mixtures. The color intensity of the obtained solid was compared. The tolerant limit was determined in case of potential interference.

2.1.7 The digital-image colorimetry procedure

For the color intensity measurement, the solid was separated from the mixture by centrifugation. The AgNPs-HAP was then redispersed with a small volume of milliQ water (≈100 μL). By using a dropper, the solid was spread onto a filter paper (Johnson test paper, No.1) cut into a circular shape with a diameter of 0.6 mm. The material on the paper support was placed in a studio box (Udio Box, 40 cm × 40 cm × 40 cm) with controlled brightness. Photos of the material was taken using a smartphone (Samsung galaxy A5, 2016 SM-A510FD) with fixed distance between the material and the smartphone (15 cm). The color intensity of the material (blue values) was determined by Image-J software as blue value in RGB mode.

2.1.8 Method validation

The performance of the proposed method was evaluated under the optimized conditions. The method figures of merit including linear range, detection limit, accuracy, and precision were determined. The method was further applied to water sample analysis. Moreover, results obtained from this method were compared with the 2,4-dinitrophenylhydrazine method using HPLC.

Under the optimized condition of the proposed method, the silver-doped hydroxyapatite was prepared by stirring 40 mg of hydroxyapatite with 1.00 mL of silver ions solution (100 mg L⁻¹). After centrifugation, the obtained Ag-HAP was immediately mixed with 5.00 mL of standard formaldehyde solution or water samples and the mixture was stirred for 30 min. Then, the obtained solid was separated from the mixture solution and the solid was redispersed in a small volume of milliQ water. After that, the solid was spread on the filter paper and its photo was

taken by a smartphone following as described in the topic 2.1.7. The color intensity of the material was determined by Image-J software and compared to that of the blank (equation 2.3).

For standard HPLC method [8], formaldehyde was mixed with 2,4-dinitrophenylhydrazine (2,4-DNP) to produce formaldehyde derivatization before the separation by the chromatographic method. For preparation of 2,4-DNP reagent, 0.06 mg of 2,4-DNP was dissolved in 20 mL of orthophosphoric acid. Then, 0.5 mL of the reagent was mixed with 5.00 mL of formaldehyde solution and 4 mL of acetonitrile. After that, the mixture was stirred for 90 min and filtrated with a 0.22 μm nylon filter. For formaldehyde analysis, 10 μL of sample solution was injected and analyzed with a reverse phase column ZORBAX Eclipse XDB-C18 (Agilent, 4.6 mm i.d. x 150 mm length column) with the temperature of column oven at 35 $^{\circ}\text{C}$. The sample solution was separated using methanol/water as a mobile phase in gradient mode at a flow rate of 1 mL min^{-1} . In gradient mode, the ratio of methanol/water was set at 50/50 and risen to 90/10 v/v in 3 min. Then, this ratio was decreased back to 50/50 v/v in 4 min, and kept for 1 min. After the separation, the formaldehyde derivative was detected at 350 nm. Under this condition, the linear range was observed in the range of 30-200 $\mu\text{g L}^{-1}$ with a limit of detection (LOD) and limit of quantification (LOQ) of 10 and 24 $\mu\text{g L}^{-1}$, respectively.

a. Calibration curve and linearity

In this part, the linearity of the method was determined in the concentration range of 15-200 $\mu\text{g L}^{-1}$. All formaldehyde standard solutions were analyzed by the Ag-HAP method under the optimized condition. The obtained ΔI was used to construct an external standard calibration curve against formaldehyde concentrations.

b. Accuracy and precision in sample analysis

To evaluate the method accuracy in sample analysis, the spiked sample method was adopted. In addition, the results obtained from the Ag-HAP method in samples and spiked sample analysis were compared to the results from the 2,4-dinitrophenylhydrazine method using HPLC.

Four water samples were collected including drinking water samples from local supermarket in Bangkok (Thailand), a simulated runoff water from fishpond containing drug for parasitic infection control, and residual waste of reagent for specimen preservation from a biology laboratory. Water samples were spiked to contain 20, 50, or 100 $\mu\text{g L}^{-1}$ formaldehyde. Then all samples were analyzed according to the procedure described previously. The obtained results from non-spiked water samples and spiked water samples analysis were compared to the external standard calibration curve to determine formaldehyde concentrations. Then, analyte recovery (%recovery) was calculated using equation 2.4. The precision of the method was evaluated by calculating the percent relative standard deviation (%RSD) of the results.

$$\% \text{recovery} = \frac{(X_s - X_{ns})}{S} \times 100\% \quad (2.4)$$

X_s is the concentration of formaldehyde found in spiked sample

X_{ns} is the concentration of formaldehyde found in non-spiked sample

S is the concentration of formaldehyde spiked in the sample

2.2 Results and discussion

2.2.1 Characterization of materials

a. X-ray diffraction (XRD)

The product obtained from co-precipitation between $\text{Ca}(\text{NO}_3)_2$ and H_3PO_4 solution was characterized by XRD (2θ range from 10° to 60°) to identify the crystalline structure. The XRD pattern of the obtained material was compared with the standard pattern of hydroxyapatite (JCPDS card 9-0432) as shown in Figure 2.2. The XRD pattern of material corresponded to hexagonal structure, and it showed the same characteristic diffraction peaks as that of hydroxyapatite (2θ at 26.0° , 31.9° , 32.1° , and 32.9°) [35]. Therefore, the results confirmed that the hydroxyapatite was obtained.

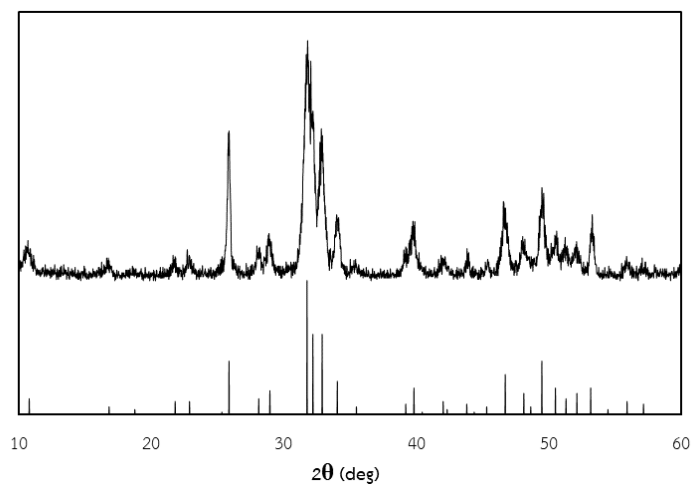


Figure 2.2 XRD pattern of the hydroxyapatite prepared by co-precipitation method compared to JCPDS card 9-0432 (below).

b. Transmission electron microscopy (TEM)

The morphology of the hydroxyapatite before and after formaldehyde detection was observed by TEM as shown in Figure 2.3. The TEM images revealed the rod-shaped particles of prepared hydroxyapatite with a size of approximately 50-80 nm (Figure 2.3A). After formaldehyde detection, spherical silver nanoparticles were observed on the material (Figure 2.3B), confirming that the chemical reduction of silver by formaldehyde occurred on the hydroxyapatite surface.

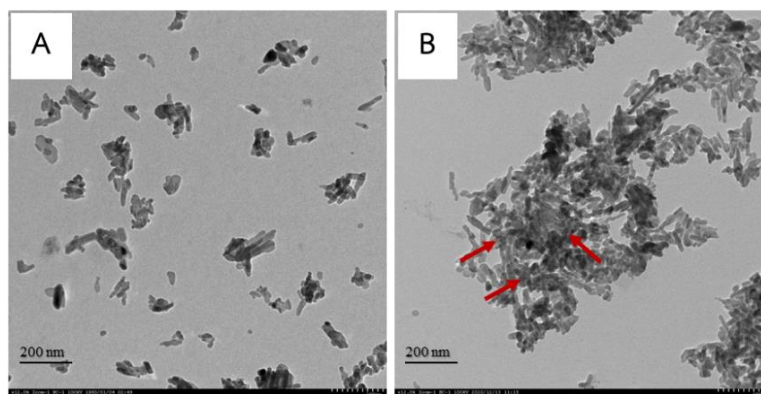


Figure 2.3 TEM images of hydroxyapatite (A) before formaldehyde detection and (B) after the detection of $50 \mu\text{g L}^{-1}$ formaldehyde. Red arrows highlight silver nanoparticles on the surface.

c. X-ray photoelectron spectroscopy (XPS)

The X-ray photoelectron spectroscopy (XPS) was used to investigate the silver species on the material surface after chemical reduction with formaldehyde. In Figure 2.4, the XPS spectrum of hydroxyapatite after the detection of formaldehyde showed two peaks at binding energy of 368 eV and 373.5 eV, attributed to the binding energy of Ag 3d $5/2$ and Ag 3d $3/2$, respectively. Moreover, the deconvoluted peaks presented two peaks at 368.971 eV and 374.298 eV corresponding to elemental silver and the peaks at 367.490 eV and 373.019 eV indicated the silver of silver oxide compound [36]. Accordingly, it was confirmed that the silver nanoparticles and Ag_2O occurred on the hydroxyapatite surface after the contact with formaldehyde, indicating the chemical reduction of silver ions by formaldehyde.

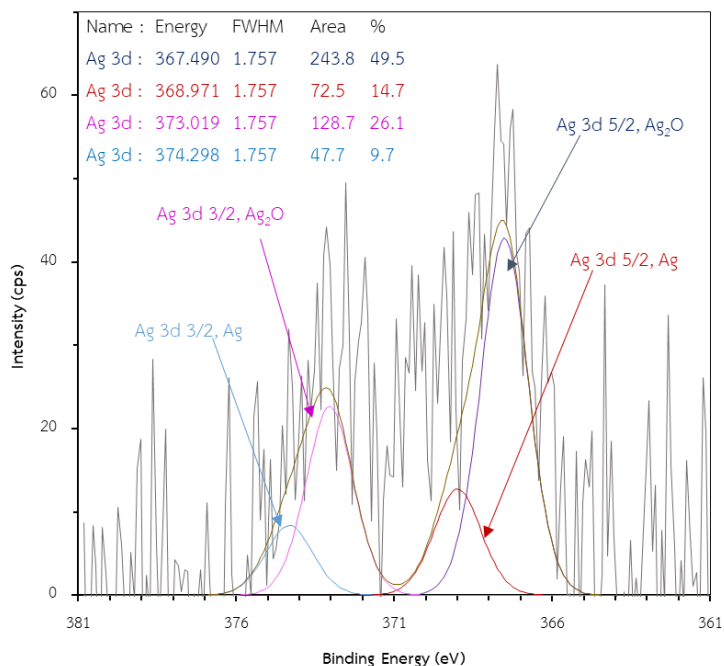


Figure 2.4 The XPS spectra of AgNPs-HAP obtained after the detection of $70 \mu\text{g L}^{-1}$ formaldehyde and corresponding deconvoluted peaks of Ag (3d).

2.2.2 Optimization of parameters for formaldehyde detection

























For the detection of formaldehyde, the effect of silver ion concentration, sodium hydroxide concentration, contact time, and sample volume on formaldehyde detection were studied. After the reaction with formaldehyde, the color of the material turned from off-white in the absence of formaldehyde to pale yellow and brown upon an increase of formaldehyde concentration. It was related to the increasing content of silver nanoparticles formed on the material. For formaldehyde quantitation, the color intensities in blue mode were collected, and the results were presented in term of ΔI , calculated by equation 2.3. Presenting the results as ΔI would emphasize on the change in material color, as it was compared to the material blank.

a. Effect of silver ion concentration

In this work, the mechanism of formaldehyde detection is based on the reducing properties of formaldehyde and the Tollens' reaction. As silver ions are the

major reactant of Tollens' reaction, the content of silver ions on hydroxyapatite would affect the sensitivity of formaldehyde detection. Hydroxyapatite (40 mg) was modified with 50 – 100 mg L⁻¹ silver ions solution (1.00 mL). The obtained materials were used in the analysis of formaldehyde standard solutions (10 - 150 µg L⁻¹) and the results are shown in Table 2.3 and Figure 2.5.

Table 2.3 The effect of silver ion concentration for HAP modification on the color of AgNPs-HAP used in formaldehyde detection.

Silver ion concentration (mg L ⁻¹)	Formaldehyde (µg L ⁻¹)							
	0	10	25	50	75	100	125	150
50								
75								
100								

In the Table 2.3, the color of obtained materials was changed from off-white in the absence of formaldehyde to pale and intense yellow, depending on the concentration of formaldehyde due to an increasing amount of silver nanoparticles. The result showed that by raising the silver ion concentration for modification on hydroxyapatite, the detection sensitivity was enhanced. The material color change could be clearly observed at 25 µg L⁻¹ of formaldehyde when increasing the silver ion concentration up to 75 and 100 mg L⁻¹. However, using very high concentration of silver ions (> 100 mg L⁻¹) resulted in pale yellow color on the blank material due to large amount of silver oxide formed on the surface when the material was mixed with the blank solution under the strong basic conditions. Consequently, the observation of color change due to silver nanoparticles formation became more difficult, reducing detection sensitivity. The color intensity of the materials was then determined, and the effect of silver ion concentration clearly manifested in Figure 2.5.

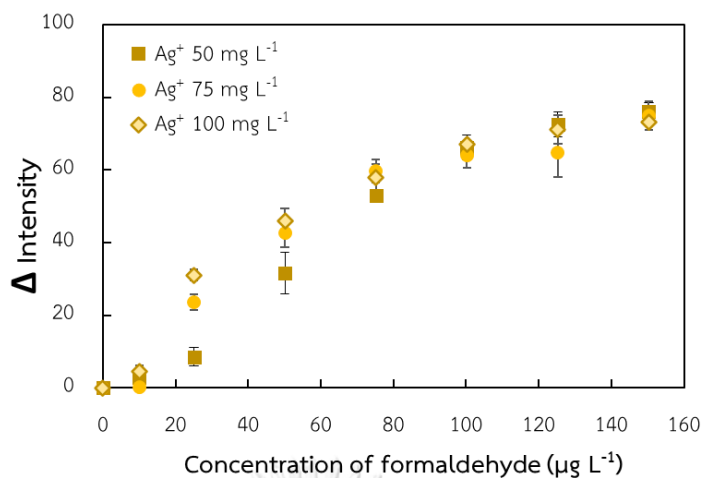


Figure 2.5 The Δ intensity of materials color observed in the detection of formaldehyde by Ag-HAP prepared by using various silver ion concentrations.

In Figure 2.5, the detection of low formaldehyde concentrations ($10\text{--}50\ \mu\text{g L}^{-1}$) was clearly enhanced as shown in increasing ΔI values when the silver ion concentration was increased. However, the effect was less pronounced in the detection of high concentration of formaldehyde ($75\text{--}150\ \mu\text{g L}^{-1}$). The result showed that the Ag-HAP prepared by using $100\ \text{mg L}^{-1}$ silver ions gave the highest detection sensitivity.

The results could be explained by the amount of silver ions adsorbed on hydroxyapatite. By increasing silver ions concentration in solution from 50 to $100\ \text{mg L}^{-1}$, the efficiency in silver ions adsorption was increased due to an increase in driving force for silver ions diffusion from bulk solution to hydroxyapatite surface [37]. Consequently, the content of silver ions adsorbed on HAP (Ag_{HAP}^+) increased from 0.97 to $1.75\ \text{mg g}^{-1}$ (Figure 2.6) and hence, the number of active sites for formaldehyde detection arose. In solution containing low formaldehyde concentrations ($10\text{--}50\ \mu\text{g L}^{-1}$), the driving force for formaldehyde diffusion to the solid surface was also low because of low concentration gradient between the bulk solution and solid surface. However, if there were plenty of silver ions on the HAP surface for the reaction, the probability for the reaction to occur was increased, and the product yield would be increased. On the other hand, this effect was less

pronounced in solutions containing high formaldehyde concentrations (75-150 $\mu\text{g L}^{-1}$) as the concentration gradient and driving force were high for the diffusion of formaldehyde from bulk to the Ag-HAP surface. Consequently, high content of AgNPs could be obtained in these conditions. Therefore, an optimum silver ion concentration of 100 mg L^{-1} was applied for preparing Ag-HAP in further experiments.

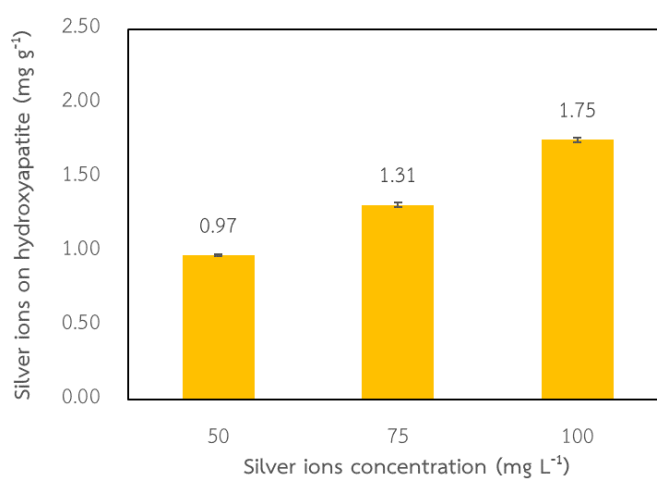


























Figure 2.6 Effect of silver ion concentrations on the efficiency of silver ions adsorption on hydroxyapatite.

b. Effect of sodium hydroxide concentration

To obtain a suitable condition for formaldehyde reaction, the concentration of sodium hydroxide in formaldehyde solutions (10-100 $\mu\text{g L}^{-1}$) was varied as 0.10, 0.15, 0.20, or 0.25 mol L^{-1} . The results are shown in Table 2.4 and Figure 2.7. It was found that when increasing the sodium hydroxide concentration in solution up to 0.25 mol L^{-1} , the yellow color of AgNPs was observed at lower concentrations of formaldehyde (10 and 25 $\mu\text{g L}^{-1}$) as shown in Table 2.4 and the ΔI value was also risen as shown in Figure 2.7. Hence, the sensitivity of the detection was improved by raising sodium hydroxide concentration. This could be explained by the major role of sodium hydroxide in Tollens' reaction. In this reaction, sodium hydroxide acts as an accelerator catalyst to react with the formaldehyde intermediates [23] and to produce silver oxide for further reduction by formaldehyde [38, 39]. Therefore,

increasing sodium hydroxide concentration would enhance the amount of catalyst for formaldehyde intermediates and the amount of silver oxide formed on the hydroxyapatite surface. A higher number of active sites on the surface resulted in a rising probability for chemical reduction. However, the working linear range was narrow when 0.20 and 0.25 mol L⁻¹ sodium hydroxide were used. Thus, 0.15 mol L⁻¹ of sodium hydroxide was chosen for the next experiments.

Table 2.4 The effect of sodium hydroxide concentration on the color of AgNPs-HAP used in formaldehyde detection.

Sodium hydroxide concentration (mol L ⁻¹)	Formaldehyde (μg L ⁻¹)					
	0	10	25	50	75	100
0.10						
0.15						
0.20						
0.25						

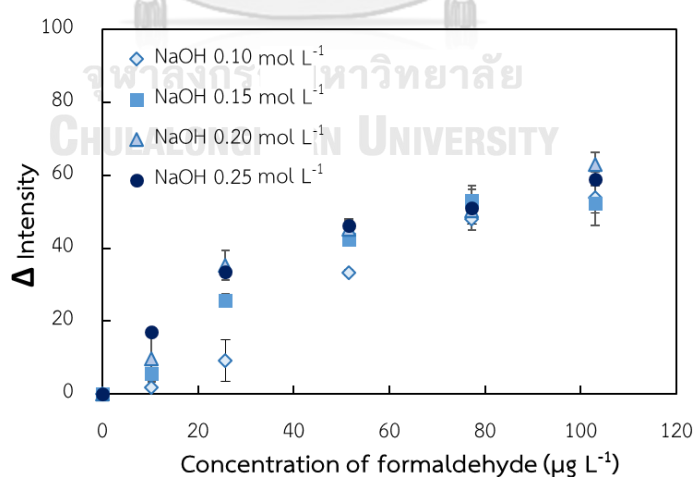




















Figure 2.7 The Δ intensity of materials color observed in the analysis of formaldehyde solutions containing different sodium hydroxide concentrations.

c. Effect of contact time

To obtain a suitable contact time that resulted in a good detection sensitivity, the contact time of 30, 60, or 90 min was applied to detect 10-100 $\mu\text{g L}^{-1}$ formaldehyde (Table 2.5 and Figure 2.8). From preliminary test, the contact time less than 30 min was not sufficient to produce quantitative amount of AgNPs, in particular in low-level formaldehyde solutions. It was found that the contact time in the studied range did not give a noticeable color difference by naked eyes (Table 2.5). When ΔI of materials was observed as shown in Figure 2.8, prolonging the contact time did not affect the ΔI of material at low-level formaldehyde detection. It indicated that a 30 min of contact time was enough for the diffusion of formaldehyde to the Ag-HAP and the chemical reduction to occur at its maximum extent. However, in high-level formaldehyde detection (50 – 100 $\mu\text{g L}^{-1}$), results from using a 30 min contact time showed an increasing trend of ΔI in increasing formaldehyde concentration, while the result from longer period did not show a significant change of ΔI . With a reaction time of 60 and 90 min, there might be a saturation of silver nanoparticles formed on the surface due to limited number of active sites compared to formaldehyde content. From the result, the contact time of 30 min was chosen as a linear relationship in the range of 10 – 100 $\mu\text{g L}^{-1}$ formaldehyde was obtained.

Table 2.5 The effect of contact time on the color of AgNPs-HAP used in formaldehyde detection.

Contact time (min)	Formaldehyde ($\mu\text{g L}^{-1}$)					
	0	10	25	50	75	100
30						
60						
90						

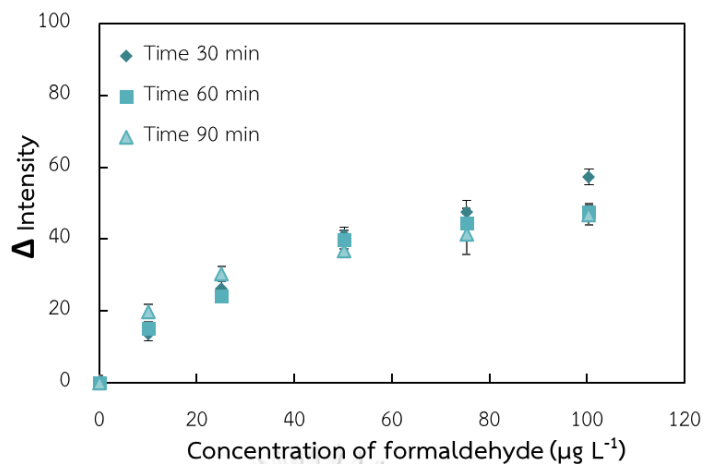


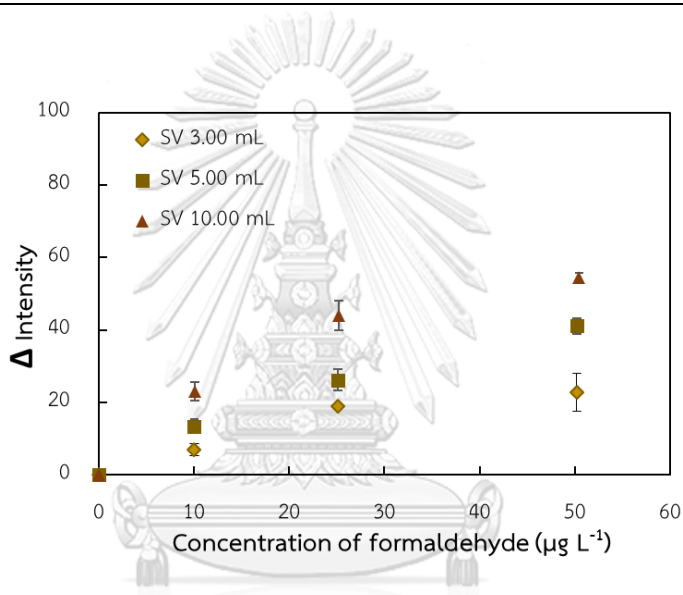
Figure 2.8 The Δ intensity of Ag-HAP color observed by using different contact times for detection of formaldehyde.

d. Effect of sample volume

To improve the detection sensitivity, the sample volume was increased from 3.00 to 10.00 mL. The detection of low levels of formaldehyde ($10\text{-}50 \mu\text{g L}^{-1}$) was focused in this study (Table 2.6 and Figure 2.9). The results showed that the detection sensitivity was improved by increasing the sample volume from 3.00 to 10.00 mL as the change of material color could be better observed. The ΔI value also showed a harper increasing trend when increasing formaldehyde concentration. This could be explained by a raise of analyte mass for the detection. Despite a high sensitivity obtained by using 10.00 mL sample volume, it showed extremely narrow linear relationship ($10\text{-}25 \mu\text{g L}^{-1}$) and the result trend declined afterward, probably due to a saturation of AgNPs on Ag-HAP caused by limited active sites. On the other hand, the use of 5.00 mL sample volume provided a good detection sensitivity and a wider linear range for low-level formaldehyde detection. This sample volume was chosen for this method.

Table 2.6 The color of Ag-HAP observed with various of sample volume.

Sample volume (mL)	Formaldehyde ($\mu\text{g L}^{-1}$)			
	0	10	25	50
3.00				
5.00				
10.00				

**Figure 2.9** The Δ intensity of Ag-HAP color observed by using different sample volumes.

2.2.3 Selectivity test

In this work, this proposed method was used to detect formaldehyde based on the reducing properties of aldehyde with Tollens' reaction. This reaction is generally used to distinguish aldehydes from ketones. In this study, the effect of compounds with different functional groups (i.e. acetone, acetic acid, ethanol, and formic acid) and salts commonly found in water (i.e. sodium phosphate, sodium chloride, and sodium sulfate) were investigated in single compound solutions (Figure 2.10A) and binary mixture systems (Figure 2.10B). The selectivity of this method was

evaluated by comparing the ΔI of the material obtained from the analysis of formaldehyde solution in the absence and in the presence of the investigated compound. The results shown in Figure 2.10 were the signal observed at the tolerant limit of each compound.

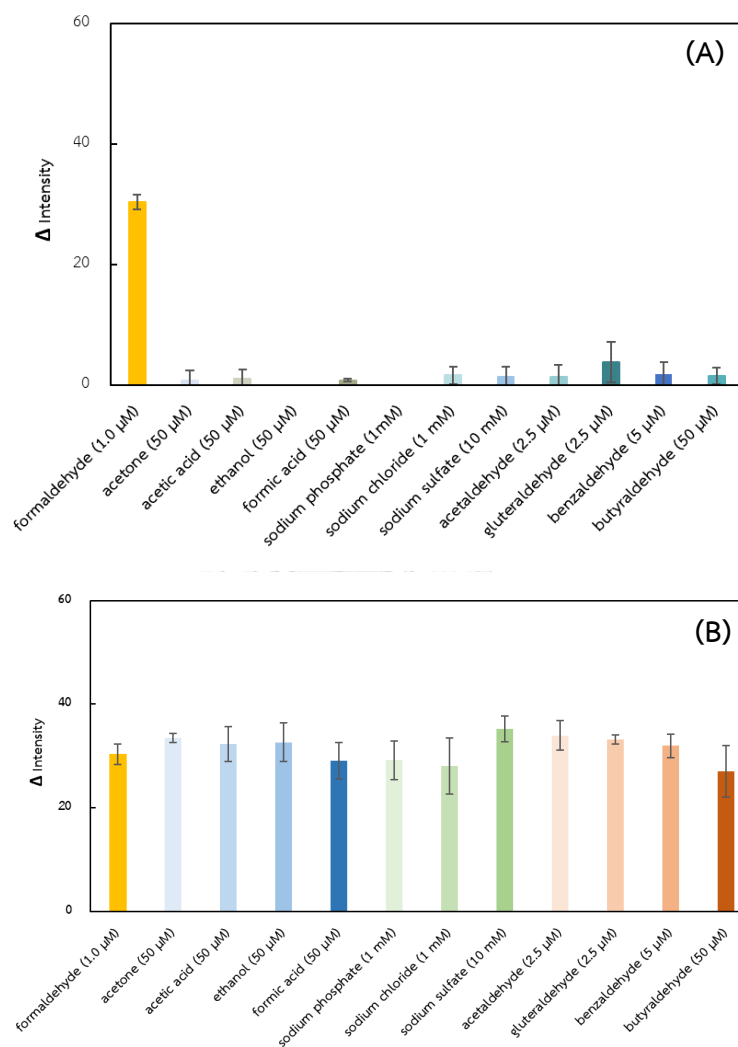


Figure 2.10 The Δ intensity of Ag-HAP color observed in the detection of (A) formaldehyde and various compounds (B) formaldehyde in the absence (only formaldehyde) and in the presence of various compounds.

Apparently, acetone, acetic acid, ethanol, formic acid, and sodium sulfate in solution at the studied concentration did not give a significant change of signals as

shown in the Figure 2.10. The presence of sodium chloride and sodium phosphate at a level higher than 1 mmol L^{-1} resulted in a pale gray material due to the formation of silver chloride and silver phosphate. The signal from formaldehyde $1.0 \text{ } \mu\text{mol L}^{-1}$ was not significantly different from the signal from binary mixture containing sodium chloride or sodium phosphate using paired t-test at a 95% of confidence-level. Thus, the method showed a tolerant limit of 1 mmol L^{-1} for sodium chloride and sodium phosphate.

To investigate the selectivity of the method toward formaldehyde detection over the other aldehydes, acetaldehyde, butyraldehyde, benzaldehyde, and glutaraldehyde were chosen in this study. It was found that $50 \text{ } \mu\text{mol L}^{-1}$ of butyraldehyde did not affect the determination of formaldehyde while acetaldehyde, glutaraldehyde, and benzaldehyde showed strong interfering effect. The presence of acetaldehyde, glutaraldehyde at a level higher than $2.5 \text{ } \mu\text{mol L}^{-1}$ and benzaldehyde at a level higher than $5.0 \text{ } \mu\text{mol L}^{-1}$ resulted in a positive error in formaldehyde determination.

This could be explained by the reducing power of the aldehydes. Adkins and co-worker [40] reported the oxidation potential of different types of aldehydes. It was demonstrated that the structure of aldehydes would affect their reducing power, and hence showed different oxidation potentials. The lower oxidation potential was observed given by the replacement of hydrogen on the alkyl group of aldehydes, a long chain alkyl, or an aryl group, as a result, formaldehyde has the highest this value. Therefore, formaldehyde is the best reducing agent compared to the other structures. Among the aldehydes used, the oxidation potential of acetaldehyde and glutaraldehyde were closed to that of formaldehyde. For this reason, acetaldehyde, and glutaraldehyde manifested strong interfering effect in formaldehyde detection.

Fortunately, these interfering aldehydes are rarely present in water. From drinking water purification process, formaldehyde could be a major aldehyde found as by-product in drinking water [4, 41]. Moreover, formaldehyde was also reported to be the most found aldehyde in natural water [42]. Hence, there was a high potential for the application of this method to detect formaldehyde in low matrix interference including drinking water and natural water.

2.2.4 Method validation and sample analysis

For the determination of formaldehyde by silver-doped hydroxyapatite method, the linear relationship between ΔI of materials color and formaldehyde concentrations was observed in a concentration range of 15 – 200 $\mu\text{g L}^{-1}$. The calibration curve is shown in Figure 2.11 and the observed color of AgNPs-HAP materials is also presented.

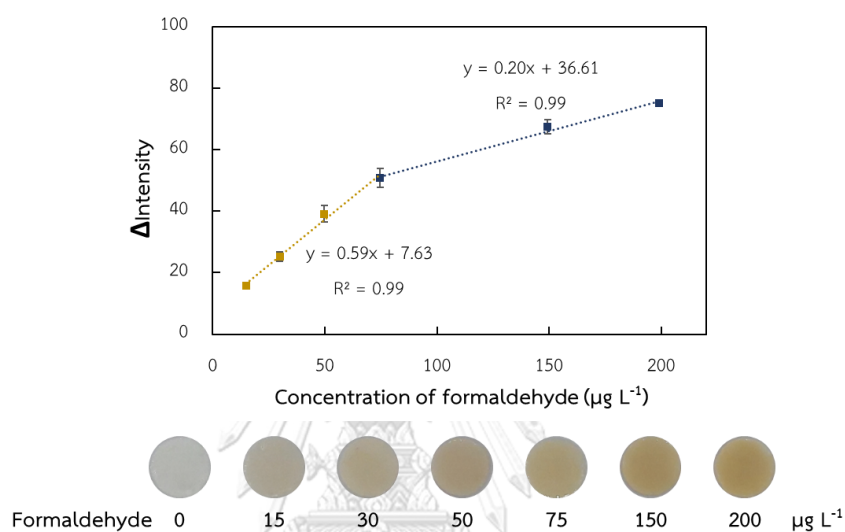


Figure 2.11 The calibration curve for formaldehyde determination and the observed materials color after formaldehyde detection.

The linear calibration curve could be divided into two ranges of concentrations depending on the sensitivity. The first concentration range was from 15-75 $\mu\text{g L}^{-1}$ with a linear relationship of $y = 0.59x + 7.63$ ($R^2=0.99$), the second range was from 75-200 $\mu\text{g L}^{-1}$ with a linear relationship of $y = 0.20x + 36.61$ ($R^2=0.99$). The percent relative standard deviation (%RSD) of the calibration curves slope was less than 7% when repeated inter-day and the lowest concentration for formaldehyde detection by this method was 15 $\mu\text{g L}^{-1}$.

From the linear range, higher sensitivity was obtained in the detection of low levels of formaldehyde (15 – 75 $\mu\text{g L}^{-1}$) and the sensitivity of the detection declined afterward. In high-level formaldehyde solutions, large content of silver nanoparticles was produced on the material and the material turned brown or dark brown. In term

of color intensity, blue values obtained from brown or dark brown color were very close. Consequently, the color intensity did not change much despite a sharp change of formaldehyde concentration, lowering the detection sensitivity in this concentration range. The proposed method was further used to determine the level of formaldehyde in various water samples as shown in Table 2.7.

Table 2.7 Results from water sample analysis using the silver-doped hydroxyapatite method and the HPLC method.

Samples	Added ($\mu\text{g L}^{-1}$)	This method			HPLC method		
		Found ^a	%Recovery	%RSD	Found ^a	%Recovery	%RSD
Drinking water sample 1	-	n.d.	-	-	n.d.	-	-
	50	49 \pm 3	98	6	51 \pm 2	101	3
	100	86 \pm 7	86	8	103 \pm 6	103	6
Drinking water sample 2	-	n.d.	-	-	n.d.	-	-
	50	53 \pm 4	107	7	52 \pm 3	105	5
	100	111 \pm 4	111	4	105 \pm 4	105	4
Residual waste from biological laboratory	-	42 \pm 3	-	-	40 \pm 5	-	-
	20	62 \pm 2	99	3	61 \pm 1	104	2
	100	138 \pm 5	96	3	136 \pm 8	96	6
Simulated fishpond runoff	-	42 \pm 3	-	-	37 \pm 1	-	-
	20	61 \pm 2	98	3	58 \pm 2	102	3
	100	139 \pm 9	97	6	131 \pm 9	94	7

n.d. = not detectable

^a mean \pm SD (n = 3)

The accuracy of the method was evaluated by comparing the results to those obtained by the HPLC method with formaldehyde derivatization with 2,4-dinitrophenylhydrazine and the recovery of formaldehyde in spiked samples. The concentration of formaldehyde in different samples determined by the silver-doped hydroxyapatite method were not significantly different from the values determined by HPLC method at a 95% confidence level. The developed method produced results with %recovery in the range of 86-111%, compared to 94-105% by HPLC method. %RSD indicating the precision of the results observed by using the proposed

method was less than 8%, compared to 7% by HPLC method. From the AOAC guideline [43], the recommended recovery and %RSD of the analytical results in the determination of analyte at $100 \mu\text{g L}^{-1}$ level was 80-110% and not higher than 15%, respectively. Therefore, these results revealed that the developed method could produce results with good accuracy and precision.



CHAPTER 3

COLORIMETRIC DETERMINATION OF FORMALDEHYDE USING AGAR-HPMC COMPOSITE GEL MODIFIED WITH SCHIFF'S REAGENT

In this part, a colorimetric method is proposed for detecting formaldehyde in water samples using agar-HPMC gel modified with Schiff's reagent (Schiff-gel). Formaldehyde diffused to react with Schiff's reagent inside the Schiff-gel, yielding a product of magenta color on the gel. The reaction between formaldehyde and Schiff's reagent was occurred following the Figure 1.1. The colorimetric detection was achieved by observing the gel color change, observed by naked eyes and the color intensity was measured with Image-J software.

3.1 Experiments

3.1.1 Apparatus

Table 3.1 List of analytical apparatus.

Apparatus	Manufacturing/Models
Hot plate	IKA/C-MAG HS7
Magnetic stirrer	GEM/MS101
pH meter	Mettler TOLEDO/Seven compact model
UV-visible spectrophotometer	Hewlett Packard/HP 8453
Vortex Mixer	Scientific Industries/GENIE2

3.1.2 Chemicals and reagent

Table 3.2 List of chemicals.

Chemicals	Supplies
Agar powder (food grade)	Telephone Agar
Formaldehyde (40% w/v)	Carlo Erba
Hydrochloric acid	Merck
Hydroxypropyl methylcellulose (HPMC)	Soap Lab
Nitric acid (HNO ₃)	Merck

Table 3.2 List of chemicals. (Cont.)

Chemicals	Supplies
Phosphoric acid (H ₃ PO ₄)	Carlo Erba
Rosaniline hydrochloride	BDH laboratory reagents
Sodium bicarbonate (NaHCO ₃)	Merck
Sodium hydroxide (NaOH)	Merck
Sodium sulfite (Na ₂ SO ₃)	Merck

All chemicals were of analytical grade and used without further purification. The reagents were prepared by using milliQ water as described as followed.

Formaldehyde solution

A 1000 mg L⁻¹ formaldehyde standard solution was prepared and used as a stock solution by diluting 40% (w/v) formaldehyde with milliQ water. The concentration of formaldehyde solution was determined by the titration method [31-33] as presented in Chapter 2 (2.1.3).

Schiff's reagent solution

A 2.50 mmol L⁻¹ of Schiff's reagent solution was prepared by dissolving 0.0210 mg of rosaniline hydrochloride, 0.1000 g of sodium sulfite, and 0.100 mL of hydrochloric acid in milliQ water. Then, 2 mL of phosphoric acid was added into the mixture. The final volume was adjusted to 25.00 mL by milliQ water. The reagent solution was freshly prepared before use.

3.1.3 Preparation of Schiff-gel

The material was prepared by dissolving 0.200 g of agar powder and 0.300 g of HPMC in 20 mL of milliQ water. The mixture was stirred and heated until the solution become clear and colorless. Then, 4.50 mL of this mixture was diluted with 4.50 mL of milliQ water and 1.00 mL of Schiff's reagent was added to this solution dropwise under continuous stirring. After that, 0.200 mL of the obtained mixture was dropped on the lid of the centrifuge tube (0.3 cm high x 0.8 cm i.d.). Finally, the Schiff-gel was obtained after keeping the mixture at 4 °C in a refrigerator for 1 hr.

3.1.4 Detection of formaldehyde

The obtained Schiff-gel on the lid of centrifuge tube was washed with milliQ water before use for formaldehyde detection. For the detection, 2.00 mL of formaldehyde solution was pipetted into the centrifuge tube with Schiff-gel on the lid. After closing the lid, the centrifuge tube was shaken by a vortex mixer for a specific period. Then, the solution was discarded, and the photo of the obtained Schiff-gel was taken by a smart phone (Samsung galaxy note 10+) in a studio box with controlled brightness and distance between the material and smartphone (10 cm). The photo was subjected to Image-J software to measure the color intensity in RGB mode, and the green values were collected. The formaldehyde detection procedure is schematically shown in Figure 3.1.

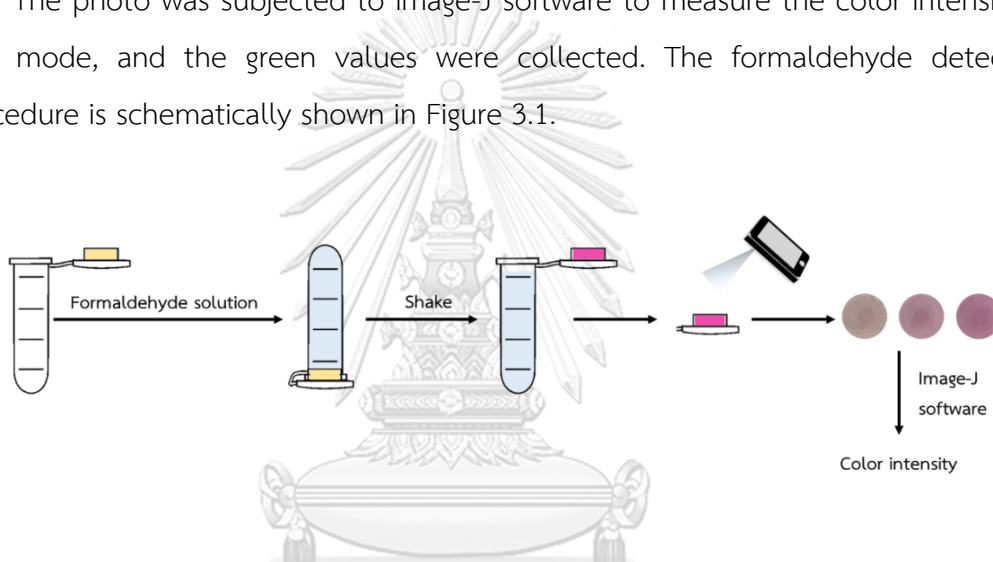


Figure 3.1 The analytical procedure for formaldehyde detection by Schiff-gel.

a. Effect of Schiff's reagent concentrations

To obtain a suitable Schiff's reagent concentration for formaldehyde detection, Schiff's reagent solutions of different concentrations ranging from 1.00 to 2.50 mmol L⁻¹ were prepared by diluting a 2.50 mmol L⁻¹ Schiff's reagent solution with milliQ water. Then, 1.00 mL of diluted Schiff's reagent solution was mixed with agar-HPMC mixture. The obtained Schiff-gel was further used to detect formaldehyde (2.00 – 10.00 mg L⁻¹) as described previously. The contact time used in this experiment was 15 min. The suitable Schiff's reagent concentration for this method was selected for the next experiment.

b. Effect of contact time

The contact time used in formaldehyde detection was varied in the range of 15 – 60 min. Formaldehyde standard solution at the concentrations of 2.00 – 10.00 mg L⁻¹ were selected for this experiment. The Schiff-gel was prepared by using 2.00 and 2.50 mmol L⁻¹ Schiff reagent to mix with the agar-HPMC mixture.

3.1.5 The digital-image colorimetry procedure

In measurement process, the lid with Schiff-gel was cut from the centrifuge tube after being in contact with a formaldehyde solution for a suitable period. The lid was placed in a studio box (Udio Box, 40 cm × 40 cm × 40 cm) with controlled brightness and the photo of the gel was captured by a smartphone (Samsung galaxy note 10+, SM-N975F/DS) with a fixed distance between the material and the smartphone (10 cm). The color intensity of the Schiff-gel was measured by Image-J software in green value of RGB mode (I). The results were present as the Δ intensity ($\Delta I = I_{\text{blank}} - I_{\text{Schiff-gel}}$) by comparing between the color intensity of the Schiff-gel tested with a blank solution (I_{blank}) and that of the Schiff-gel tested with formaldehyde ($I_{\text{Schiff-gel}}$).

3.1.6 Method performance and sample analysis

The performance of the developed method was examined under the chosen condition. The method performance including linear working range, accuracy, and precision in water sample analysis was evaluated.

a. Calibration curve and linearity

The linearity of this method was examined in the concentration range of 2.00 – 10.00 mg L⁻¹ under the chosen condition. The external calibration curve was constructed using ΔI against formaldehyde concentrations.

b. Accuracy and precision in sample analysis

The method accuracy was assessed by spiked recovery experiments. Two drinking water samples were collected from a local supermarket in Bangkok (Thailand) and two water samples were simulated runoff water from fishpond

containing drug for parasitic infection control, and residual waste of reagent for specimen preservation from biology laboratory. The suitable condition was applied to analyze the water samples. Water samples were spiked to contain 3.00 to 7.00 mg L⁻¹ formaldehyde. Then, the formaldehyde in non-spiked and spiked samples by the method. The Schiff-gel prepared from 2.50 mmol L⁻¹ of Schiff's reagent was put in contact with 2.00 mL of sample for 15 min. The obtained results were compared to an external standard calibration curve to determine formaldehyde concentration. Then, %recovery was calculated, following the equation 2.4 and precision of the method was evaluated by calculating %RSD of the results.

























3.2 Results and discussion

3.2.1 Optimization of formaldehyde detection

a. Effect of Schiff's reagent concentration

The effect of Schiff's reagent concentration was examined to find the optimal condition for formaldehyde detection. Formaldehyde standard solutions of various concentrations in the range of 2.00 – 10.00 mg L⁻¹ were used in this experiment. These formaldehyde solutions were analyzed by the Schiff-gel containing different concentrations of Schiff's reagent (1.00 – 2.50 mmol L⁻¹). The contact time between the solution and the gel was 15 min. The results are shown in Table 3.3 and Figure 3.2.

Table 3.3 The effect of Schiff's reagent concentrations on the Schiff-gel color observed in the formaldehyde detection.

Schiff's reagent concentration (mmol L ⁻¹)	Formaldehyde (mg L ⁻¹)					
	0	2.00	4.00	6.00	8.00	10.00
1.00						
1.50						
2.00						
2.50						

In Table 3.3, the color of the obtained Schiff-gel changed from pale yellow in the absence of formaldehyde to pale and intense magenta, depending on the formaldehyde concentration due to an increasing amount of product from Schiff's reaction. By increasing Schiff's reagent concentration on the Schiff-gel, the detection sensitivity was enhanced. The change of gel color could be observed at a lower formaldehyde concentration (2.00 mg L⁻¹) using Schiff-gel prepared with 1.50 – 2.50 mmol L⁻¹ Schiff's reagent. However, the starting Schiff-gel color prepared by high Schiff's reagent concentration was yellow, and it affected the color observation due to strong background color. The results could be expressed more clearly by calculating Δ color intensity of the Schiff-gel ($\Delta I = I_{\text{blank}} - I_{\text{Schiff-gel}}$) using Image-J software as shown in Figure 3.2. The color intensity observed as green values was high when the gel color was colorless or very pale yellow. When the gel turned pink or magenta, lower green values were observed.

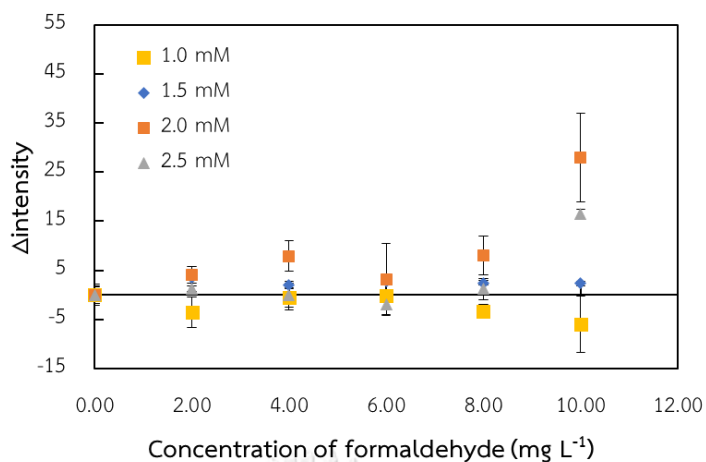


Figure 3.2 The Δ intensity of agar-HPMC color after detection of formaldehyde with various of Schiff's reagent on Schiff-gel.

In Figure 3.2, the results showed that increasing Schiff's reagent concentration on the Schiff-gel clearly enhanced the detection of formaldehyde at lower levels. When the content of Schiff's reagent on the gel increased, the number of active sites for formaldehyde detection also increased, raising the probability for the reaction to occur on the gel, despite low number of formaldehyde in solution. However, the dropping of ΔI was observed by using 2.50 mmol L⁻¹ Schiff's reagent. It could be explained that the pale-yellow color of the starting material had lower green value, compared to paler or colorless gel. Hence, after formaldehyde detection, the resulting ΔI was lower.

From these results, the Schiff-gel prepared by using 2.00 and 2.50 mmol L⁻¹ Schiff's reagent provided noticeable ΔI when used to detect formaldehyde solution. However, the trend of the results did not show a linear relationship. Hence, the effect of other parameters was further investigated. Therefore, the both of 2.00 and 2.50 mmol L⁻¹ Schiff's reagent were chosen for the next experiment.

b. Effect of contact time

In this study, the Schiff-gel was prepared by using 2.00 and 2.50 mmol L⁻¹ of Schiff's reagent. The gels were then applied to detect formaldehyde (2.00-10.00 mg L⁻¹) at different contact times (15, 30, and 60 min). The obtained Schiff-gels are

shown in Table 3.4. In this experiment, increasing the contact time was expected to increase the number of formaldehyde moles to react with Schiff's reagent at the gel surface. Unfortunately, a prolongation of contact time from 15 min to 30 min and 60 min led to a leak of Schiff's reagent from the gel, and formaldehyde solutions turned pale pink. Consequently, the gel color faded due to the reagent loss from the gel, and hence low amount of product formed in the gel. It could be explained by the low physical property of the gel prepared with this agar-HPMC ratio. The gel could not tolerate long time shaking and started to deform.

By observing the ΔI values, the results obtained with Schiff-gel prepared with 2.00 mmol L⁻¹ Schiff's reagent (Figure 3.3A) showed an increasing trend of ΔI at 30 and 60 min contact time, despite the reagent loss. However, the linear relationship was not obtained. On the other hand, a linear increase of ΔI with formaldehyde concentration was obtained by using the Schiff-gel prepared with 2.50 mmol L⁻¹ Schiff's reagent with the contact time of 15 min (Figure 3.3B). Hence, this condition was chosen for the analysis of water samples.

Table 3.4 The effect of contact time on the color of Schiff-gel prepared with 2.00 and 2.50 mmol L⁻¹ Schiff's reagent observed in formaldehyde detection.

Contact time (min)	Formaldehyde (mg L ⁻¹)											
	Gel with 2.00 mmol L ⁻¹ Schiff's reagent						Gel with 2.50 mmol L ⁻¹ Schiff's reagent					
	0	2.00	4.00	6.00	8.00	10.00	0	2.00	4.00	6.00	8.00	10.00
15												
30												
60												

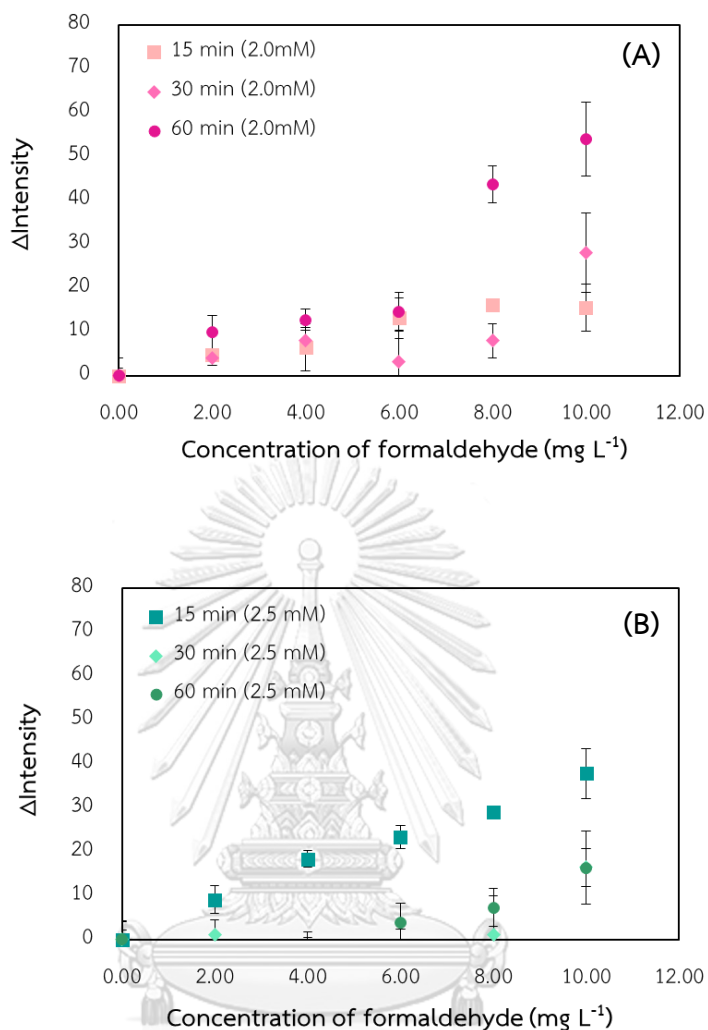


Figure 3.3 The Δ Intensity of Schiff-gel prepared with (A) 2.00 mmol L⁻¹ Schiff's reagent and (B) 2.50 mmol L⁻¹ Schiff's reagent obtained from formaldehyde detection using different contact times.

3.2.2 Method performance and sample analysis

In this part, the method performance including a linear working range and the limit of detection (LOD) was determined under the chosen conditions. The Schiff-gel was prepared by using 2.50 mmol L⁻¹ of Schiff's reagent and the Schiff-gel was put in contact with formaldehyde solution or sample for 15 min. The photo of the obtained Schiff-gel was taken by a smartphone under the controlled brightness and distance between smartphone and Schiff-gel. Then, the method was applied to water sample

analysis. The accuracy of the method was evaluated using spiked recovery experiments.

a. Calibration curve and linearity

For the determination of formaldehyde by Schiff-gel, linearity was obtained in the concentration range of 2.00 – 10.00 mg L⁻¹ (Figure 3.4). The according Schiff-gel color change is also shown. The calibration curve showed a good linear relationship with a regression equation of $y = 3.67x + 2.97$ and correlation coefficient (R^2 value) of 1.00. The relative standard deviation (%RSD) of the calibration curves slope was less than 5% when repeated inter-day. The limit of detection (LOD) of this method was calculated based on the standard deviation (σ) of the ΔI of blank analysis (n=10). The LOD was found to be 1.49 mg L⁻¹.

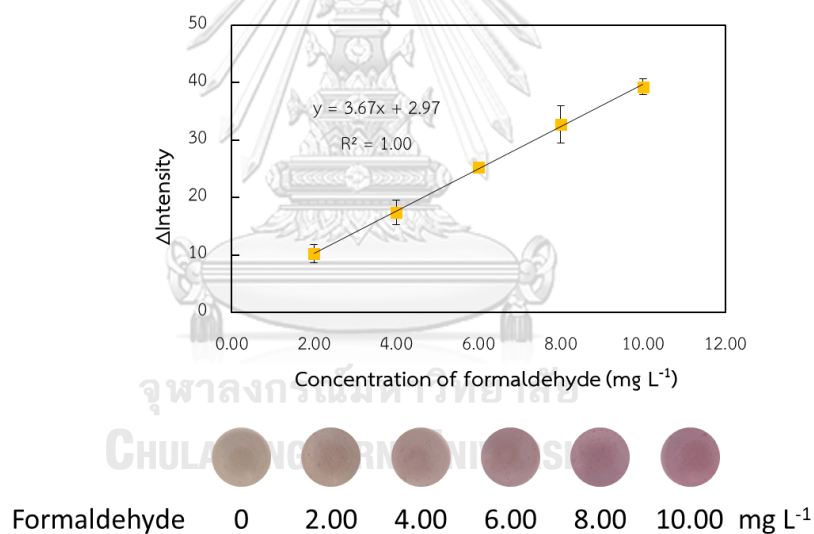


Figure 3.4 The calibration curve for formaldehyde determination and the observed color of Schiff-gel after formaldehyde detection.

b. Water samples analysis

Water samples were collected and analyzed by the chosen conditions. The accuracy of the method was assessed by spiked recovery experiments. The samples were spiked with a standard solution to contain 3.00 or 7.00 mg L⁻¹ formaldehyde.

The accuracy and precision of the method are shown in term of %recovery and %RSD of the results, respectively. The results are shown in Table 3.5. The proposed method presented %recovery and % RSD in the range of 81 - 122% and 3 to 16%, respectively. According to the AOAC criteria [43], the %recovery and %RSD in the range of 80 to 110% and 7% are suggested for the determination of analyte of 10 mg L⁻¹ level. The results showed that the accuracy and precision of the method need to be improved.

Table 3.5 Analytical results and recoveries of formaldehyde determination in water samples by the proposed method.

Water sample	Added (mg L ⁻¹)	Found ^a	%Recovery	%RSD
	-	n.d.	-	-
Drinking water sample 1	3	3.10±0.10	103	3
	7	7.93±1.26	113	16
	-	n.d.	-	-
Drinking water sample 2	3	3.49±0.23	116	7
	7	8.56±0.66	122	8
	-	2.19±0.67	-	-
Residual waste from biological laboratory	3	5.61±0.77	114	14
	7	7.92±0.90	82	11
	-	2.58±1.03	-	-
Simulated fishpond runoff	3	5.03±0.37	81	7
	7	9.33±1.47	96	16
	-			

n.d. = not detectable

^a mean ± SD (n = 3)

The major factors that may affect the results accuracy and precision were the gel composite stability and thickness. In this work, the gel was dropped onto the lid of the tube for the convenient use. However, it was found later that the thickness of the gel on the lid was different on different areas of the lid. Unexpectedly, it strongly

affected the color intensity observed on different areas of the lid due to the transparency of the gel. By better controlling the gel amount and gel thickness, the precision and accuracy of this method would be improved. Furthermore, changing the gel composition and gel type are also recommended to improve the physical and mechanical properties of the gel to be able to tolerate the shaking force in detection step.

3.3 Comparison of method performance

Comparison of the analytical performance of the two developed methods for formaldehyde determination and the previous report is present in Table 3.6.

Table 3.6 Comparison of colorimetric methods for formaldehyde detection.

Method	Linear range (LOD)	Details	Ref.
Flow injection spectrophotometry	16.6-166.5 $\mu\text{mol L}^{-1}$ (3.33 $\mu\text{mol L}^{-1}$)	- Hantzsch reaction coupled with dispersive liquid-liquid microextraction - Sample: milk	[44]
Spectrofluorometry	0.17-3.33 $\mu\text{mol L}^{-1}$ (0.13 $\mu\text{mol L}^{-1}$)	- 5-Aminofluorescein (Fl-NH ₂) entrapped in the PVA film - Sample: vegetables, fruits, and seafood soak water	[14]
Spectrophotometry	0.1-40 $\mu\text{mol L}^{-1}$ (0.05 $\mu\text{mol L}^{-1}$)	- Gold nanoparticles (AuNPs) coupled with Tollens' reagent - Sample: standard solution	[16]
Spectrophotometry	30-50 $\mu\text{mol L}^{-1}$ (27.99 $\mu\text{mol L}^{-1}$)	- Silver nanoclusters (AgNCs) coupled with Tollens' reagent - Sample: squid and ground chicken	[17]
Spectrofluorometry	33.3-3330 $\mu\text{mol L}^{-1}$ (1.66 $\mu\text{mol L}^{-1}$)	- Chitosan-based fluorescent polymers - Sample: chicken, pork, bream and tap water	[15]

Table 3.6 Comparison of colorimetric methods for formaldehyde detection. (Cont.)

Method	Linear range (LOD)	Details	Ref.
Digital-image colorimetry	33.3- 832 $\mu\text{mol L}^{-1}$ (23.3 $\mu\text{mol L}^{-1}$)	- Acetylacetone entrapped in the biodegradable film - Sample: food	[26]
Digital-image colorimetry	4.16- 41.6 $\mu\text{mol L}^{-1}$ (4.00 $\mu\text{mol L}^{-1}$)	- Schiff reagent in an acid medium -Sample: milk	[19]
Digital-image colorimetry	6.66-39.96 $\mu\text{mol L}^{-1}$ (4.33 $\mu\text{mol L}^{-1}$)	- Chromogenic substance (4-Amino-3- hydrazino-5-mercapto-1,2,4-triazole) immobilized on paper strip - Sample: wastewater	[45]
Digital-image colorimetry	9.99 – 333 $\mu\text{mol L}^{-1}$ (3.33 $\mu\text{mol L}^{-1}$)	- Acetylacetone reagent in headspace single drop microextraction - Sample: textile, wastewater	[46]
Digital-image colorimetry	0.1-100 $\mu\text{mol L}^{-1}$ (0.03 $\mu\text{mol L}^{-1}$)	- Gold nanoprism with Tollens' reagent in headspace single drop microextraction - Sample: octopus and chicken flesh	[20]
Digital-image colorimetry	0.50-6.66 $\mu\text{mol L}^{-1}$ (0.50 $\mu\text{mol L}^{-1}$) ^a	- Tollens' reaction on silver ions modified hydroxyapatite (Ag-HAP) - Sample: drinking water, Runoff water	This work
Digital-image colorimetry	66.6 – 333 $\mu\text{mol L}^{-1}$ (49.6 $\mu\text{mol L}^{-1}$)	- Schiff's reaction on agar-HPMC modified with Schiff's reagent - Sample: drinking water, Runoff water	This work

^a Lowest concentration for formaldehyde determination

For the silver-doped hydroxyapatite method, the lowest detection concentration of this work was better than that presented in several method using spectrometer and digital-image colorimetry [15, 17, 19, 26, 44-46]. By using solid phase extraction and larger sample volume, Ag-HAP method could detect low-level formaldehyde based on Tollens' reagent without additional nanoparticles or

analytical instrument. However, the use of Schiff-gel could detect formaldehyde only at high formaldehyde levels. It was likely due to the nature of gel that despite its hydrophilicity, the penetration of formaldehyde to react with Schiff's reagent inside the gel might be much more difficult, compared to the hydroxyapatite material. However, these two proposed methods could be applied to detect formaldehyde in water samples with a smartphone or digital camera using non-toxic material (hydroxyapatite and agar-HPMC gel).



CHAPTER 4

ELECTROCHEMILUMINESCENT DETECTION OF PATHOGENS ON MICROFLUIDIC DEVICE

4.1 Introduction

4.1.1 Rationales

Pathogen is defined as a microbial that can cause consumer illness and even low concentration of pathogen in water can cause the early stage of infection in humans [1]. The prevention and identification of infectious disease from pathogen is necessary. Highly sensitive and specific detection methods are required for monitoring the pathogens. The culture-based method is the standard detection method of pathogen in hospital. However, it requires well-trained users, and the analysis time is often long. An enzyme-linked immunosorbent assay (ELISA) and polymerase chain reaction (PCR); both coupled with different detection techniques such as fluorescence, electrochemical, surface enhanced Raman scattering (SERS) or colorimetric assays have been used to quantify the concentration of pathogens [47-51]. Nevertheless, these operation processes are complicated, requiring well-trained operators, and high cost. Electrochemiluminescence (ECL) is an alternative technique which is well studied for detection of biomolecules [52, 53] and heavy metal [54]. ECL has excellent characteristics, such as rapid response, simple operation processes, and excellent sensitivity. ECL does not require an excitation source, compared to fluorescence analysis; therefore, it does not encounter the problem of auto-fluorescence or a scattered light background. Furthermore, the output signal of ECL sensor is reproducible and accurate. Several commercial ECL systems have been developed to detect many analytes for clinical screening including alpha fetoprotein (AFP), carcino-embryonic antigen (CEA), calcitonin, and ferritin [55, 56].

Recently, the paper-based ECL detection platform has attracted considerable interest because of its great potential for point of care diagnosis [55-57]. Although paper-based devices show many advantages, such as simple, low cost, portable, disposable, this device cannot perform as a conventional microfluidic device [58, 59].

Even though the cost of polymer-based microfluidic devices are more expensive, the use of polymer substrates could accommodate many available detection techniques and additional options for increasing the method sensitivity, including sample preparation, reaction, or detection part [60-62]. Moreover, the use of microfluidic chips offer advantages in fluid handling and streamlining processes in ECL lysing step [60]. Therefore, a microfluidic device coupled with ECL is an interesting option for pathogen detection.

Cryptosporidium parvum or *C. parvum*, is a water parasite, that can contaminate in drinking water and can cause cryptosporidiosis. The infection of cryptosporidiosis causes diarrhea, anorexia, vomiting, and abdominal pain [63]. Moreover, sporulated oocyst of *C. parvum* can resist the disinfection process of water treatment [64]. For prevention of *C. parvum* transmission to human, the screening of *C. parvum* in water is necessary. In this research, *C. parvum* was used as a model DNA for method development.

Immunological methods are the common method for detecting *C. parvum* in water sample [65] due to the high selectivity and sensitivity in *C. parvum* detection. Fluorescent dyestuffs [66, 67], radioisotopes [68], and enzymes [69] are commonly used as signaling reagent in these methods. To enhance the signal, liposomes can be used to encapsulate the reagents [70, 71]. Moreover, the outer of liposomes consists of phospholipids and cholesterol, hence it can be modified for specific binding with an analyte. For signal amplification, a single binding of the analyte with liposome that contains a lot of signaling molecules would result in a signal enhancement after liposomes lysing by a surfactant [70]. Herein, the liposomes were used to carry the signaling molecules for *C. parvum* assay.

In this work, we presented a sandwich hybridization assay for *C. parvum* detection by ECL for further application on a simple microfluidic chip. The optimization of assay was carried out off-chip. The schematic of the developed assay for *C. parvum* DNA is shown in Figure 4.1. For *C. parvum* detection, magnetic beads were used to separate a bound sandwich complex from solution. The surface of commercial magnetic beads was modified with streptavidin for binding with biotin on the capture DNA (cDNA). When applied in sample solution, the cDNA on the

magnetic beads will specifically bind with target DNA (tDNA). After that, a reporter probe (liposome containing $\text{Ru}(\text{bpy})_3^{2+}$) bearing binding site specific to tDNA was added. The obtained magnetic beads with a bound sandwich complex were collected for further ECL or fluorescence detection.

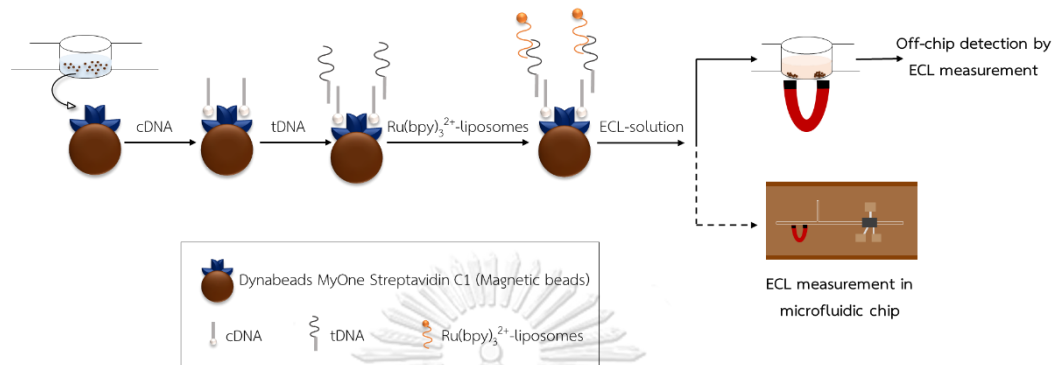


Figure 4.1 Schematic of the developed assay for *C. parvum* DNA detection by ECL.

4.1.2 Theory of this work

a. Electrochemiluminescence (ECL)

Electrochemiluminescence (ECL) is an alternative technique which is well studied for the detection of biomolecules [52, 53] and heavy metals [54]. In general, the mechanism of ECL can be divided into two pathways depending on the excited state formation mechanism. These two pathways are annihilation ECL and coreactant ECL [72, 73]. For the bioanalytical and medical applications, coreactant ECL was compatible for this field because it can be performed in an aqueous medium, under physiological conditions and in ambient air.

Tris(2,2'-bipyridine) ruthenium(II) ($\text{Ru}(\text{bpy})_3^{2+}$) is often used in ECL sensing because it is inexpensive and commercially available [74, 75]. $\text{Ru}(\text{bpy})_3^{2+}$ emits the light with a maximum emission at 620 nm (red/orange) [76]. In this work, N-butylethanol-amine (NBEA) was used as a coreactant due to the oxidation of amine. The oxidation of amine generated oxidative amine cation radicals that were further produced reductive amine free radicals after oxidation at the electrode. Meanwhile, $\text{Ru}(\text{bpy})_3^{2+}$ also underwent oxidation reaction giving intermediate $\text{Ru}(\text{bpy})_3^{3+}$ that further reacted with the amine free radicals to produce the excited

state $\text{Ru}(\text{bpy})_3^{2+*}$. The latter turned to ground state $\text{Ru}(\text{bpy})_3^{2+}$ by emitting ECL signal [77-79]. The one possible mechanism of $\text{Ru}(\text{bpy})_3^{2+}$ -ECL is shown in Figure 4.2.

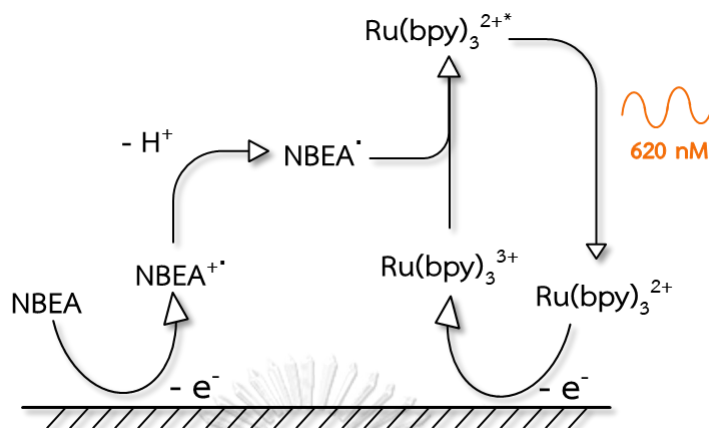


Figure 4.2 One possible mechanism of $\text{Ru}(\text{bpy})_3^{2+}$ -ECL[72].

b. Sandwich hybridization assay

Sandwich hybridization assays [80] are based on the specific binding between target DNA or RNA to capture DNA probe, complementary to a sequence in the desired target DNA. A capture probe is immobilized via functional groups and typical bioconjugation reactions on a surface. When target DNA present in the sample, the specific sequence on the capture DNA probe can bind with the target DNA. For detection part, it requires a reporter probe, which is modified with a signaling molecule such as liposomes containing signaling molecule, enzyme, or fluorophore. This reporter probe will also bind with another part of the target DNA and release signal for the detection.

c. Liposomes

In analytical field, liposomes have been used for carrying a signal enhancement receptor via encapsulation. For the detection, liposomes can be destroyed by a surfactant and the receptors are released to the detector. In this manner, the signal could be observed despite lower levels of analyte in sample [81]. Liposomes are vehicles of a spherical shape built from bilayer of phospholipid and cholesterol. It can encapsulate molecules inside the structure. Typically, liposomes are used as a carrier for delivering medicine or gene to the target cell [82].

In this work, liposomes containing $\text{Ru}(\text{bpy})_3^{2+}$ was modified with 3'-cholesteryl-TEG modified *C. parvum* reporter probe. It can bind with the target DNA as a reporter probe to amplify ECL signal. For this advantage, the trace concentrations of pathogen can be determined.

4.1.3 Objective of this work

To develop an assay for *C. parvum* DNA detection by ECL.

4.2 Experiments

4.2.1 Apparatus

Table 4.1 List of analytical apparatus.

Apparatus	Manufacturing/Models
Autolab potentiostat	Methrom/BV
Inductively coupled plasma optical emission spectroscopy (ICP-OES)	SpectroBlue/FMX36
Luminescence spectrometer	AMINCO-Bowman/Series 2 (AB2)
Laser cutting machine	VLS 2.30/Universal Laser Systems
Multi-Mode Microplate Reader	BioTek/Synergy Neo 2
Particle Size Analyzers and Zetasizers (DLS Zeta Potential Measurement)	Malvern/Zetasizer Nano-ZS
Vortex Mixer	Scientific Industries/GENIE2

4.2.2 Chemicals and reagent

Table 4.2 List of chemicals and materials.

Chemicals and materials	Supplies
1,2-dipalmitoyl-sn-glycero-3-phosphocholine (DPPC)	Avanti Polar Lipids
1,2-dipalmitoyl-sn-glycero-3-phospho-(1'-rac-glycerol) sodium salt (DPPG)	Avanti Polar Lipids
2-amino-2-(hydroxymethyl)propane-1,3-diol (Tris)	Affymetrix

Table 4.2 List of chemicals and materials. (Cont.)

Chemicals and materials	Supplies
2-[4-(2-hydroxyethyl)piperazin-1-yl]ethanesulfonic acid (HEPES)	VWR
3'-cholesteryl-TEG modified <i>C. parvum</i>	metabion
Bovine serum albumin fraction V (BSA)	Merck
<i>C. parvum</i> capture probe, biotin-mod. (cDNA)	metabion
<i>C. parvum</i> target (tDNA)	metabion
Copper adhesive tape	Plano GmbH
Conductive silver paint	Busch
Chloroform	VWR
Cholesterol	Sigma-Aldrich
D(+)-sucrose	Merck
Disodium hydrogenphosphate dihydrate	Merck
DuPont Kapton HN foil of 125 μm thickness	CMC Klebetechnik
Ethylenediaminetetraacetic acid disodium salt (EDTA)	Sigma-Aldrich
Ficoll 400	Carl Roth
Formamide	Merck
Hydrochloric acid (0.1 mol L ⁻¹)	VWR
Dynabeads MyOne Streptavidin C1 (Magnetic beads)	Thermo Fisher Scientific
Methanol	VWR
N-butyl-diethanolamine (NBEA)	Sigma-Aldrich
Poly(methyl methacrylate) (PMMA) (Plexiglas XT)	Kunststoff Acryl Design
Potassium chloride	neoFroxx
Potassium dihydrogenphosphate	Merck
Sodium azide	Merck
Sodium citrate dihydrate	Sigma-Aldrich
Sodium hydroxide solution (0.1 mol L ⁻¹)	Merck

Table 4.2 List of chemicals and materials. (Cont.)

Chemicals and materials	Supplies
Thick double-sided adhesive tape	3M
Tris(2,2'-bipyridine) ruthenium(II) dichloride hexahydrate (Ru(bpy) ₃ Cl ₂)	Sigma-Aldrich
TWEEN 20	Sigma-Aldrich
Zonyl FSN-100 fluorosurfactant	Sigma-Aldrich

Table 4.3 The sequences of all *C. parvum* probes for this work.

Type	Sequence (5' → 3')
<i>C. parvum</i> capture probe, biotin-mod. (cDNA)	[biotin]-AGA TTC GAA GAA CTC TGC GC
<i>C. parvum</i> target (tDNA)	AAG GAC CAG CAT CCT TGA GTA CTT TCT CAA CTG GAG CTA AAG TTG CAC GGA AGT AAT CAG CGC AGA GTT CTT CGA ATC TAG CTC TAC TGA TGG CAA CTG A
<i>C. parvum</i> reporter probe	GTG CAA CTT TAG CTC CAG TT-[TEG cholesteryl]

All chemicals were used without further purification and were prepared in milliQ water.

Tris-HCl buffer:

A 0.1 mol L⁻¹ Tris-HCl solution was prepared by dissolving 64 g of Tris in 1000 mL of milliQ water. The pH of solution was adjusted to 8.5 using 0.1 mol L⁻¹ HCl solution.

1xBinding & Washing (1xB&W) buffer

A 100 mL of 1xB&W buffer was prepared by dissolving 0.32 g of Tris in milliQ water. Then, 14.61 g of EDTA and 5.84 g of sodium chloride were added to the solution. This solution pH was adjusted to 7.5 using 0.1 mol L⁻¹ HCl solution.

2xBinding & Washing (2xB&W) buffer

A 100 mL of 2xB&W buffer was prepared by dissolving a 0.64 g of Tris in milliQ water. Then, EDTA 29.22 g and sodium chloride 11.69 g were added into the solution. This solution pH was adjusted to 7.5 by using 0.1 mol L⁻¹ HCl solution.

Hybridization buffer

A 100 mL of hybridization buffer was prepared by dissolving 9.06 g of sodium chloride and 3.48 g of sodium citrate dihydrate in milliQ water. Then, 0.01 g of sodium azide, 30.0 mL of formamide, and 0.2 mL of Ficoll 400 were added to the solution. Finally, this solution pH was adjusted to 7.0.

HEPES-saline-sucrose buffer (HSS buffer)

A 1000 mL of HSS buffer was prepared by dissolving 2.38 g of HEPES and 11.7 g of sodium chloride in milliQ water. Then, 0.1 g of sodium azide and 86 g of sucrose were added to the solution. Finally, this solution was adjusted the pH to 7.5.

Phosphate Buffered Saline (PBS buffer)

PBS buffer was prepared by dissolving 4.00 g of sodium chloride, 0.10 g of potassium chloride, 0.71 g of disodium hydrogenphosphate dihydrate, and 0.12 g of potassium dihydrogenphosphate in 500 mL of milliQ water. The pH of the solution was adjusted to 7.4 by using 0.1 mol L⁻¹ HCl solution.

Washing buffer

100 mL of PBS buffer was prepared by dissolving 0.01 g of BSA and 0.05 mL of Tween20 in milliQ water.

Zonyl-100 solution

5 g of Zonyl FSN-100 was dissolved in Tris-HCl buffer.

ECL lysing cocktail (ECL-solution)

One milliliter of cocktail solution was freshly prepared by mixing 33 μ L of potassium chloride, 1 μ L of NBEA, and 20 μ L of Zonyl-100 solution. The volume of the mixture was adjusted to 1 mL by Tris-HCl buffer.

Ru(bpy)₃²⁺-liposomes preparation

Liposomes were prepared by following the protocol proposed by Edwards and co-workers [82]. In brief, 30 mg of DPPC, 15 mg of DPPG, and 19 mg of cholesterol were added into the solution of 3 mL chloroform and 0.5 mL methanol. Next, 50 μ L of 3'-cholesteryl-TEG modified *C. parvum* reporter probe (300 μ mol L⁻¹) was added into the liposome mixture and sonicated for a few seconds at 50 °C. Then, 2 mL of solution containing Ru(bpy)₃Cl₂ (100 mmol L⁻¹) in 0.2 mol L⁻¹ HEPES (pH 7.5) was added into the obtained solution and sonicated for 5 min. The organic

solvent in the mixture was removed using a rotary evaporator. After evaporation, 2 mL of the 3'-cholesteryl-TEG modified *C. parvum* reporter probe was added into the obtained mixture and vortexed for 5 min with short reheating steps to keep the obtained lipid dispersion above the phase transition temperature (55 °C). Before the purification of liposomes, the lipid dispersion was extruded through polycarbonate membranes (0.4 µm and 0.2 µm) for 21 times while keeping the temperature of lipid dispersion at 55 °C. For the purification of liposomes, the obtained dispersion was separated on a Sephadex G-50 medium column. After that, the obtained dispersion was packed in dialysis kit (Spectrum Labs Spectra/Por standard tubing dialysis membrane, molecular cut-off 12-14 kDa) and dialysis was performed in HSS buffer overnight. The obtained liposomes were stored at 4 °C and protected from light. The obtained liposomes were characterized by DLS Zeta Potential to observe the size distribution and zeta potential. The phospholipid concentration was determined by ICP-OES.

4.2.3 Assay with magnetic beads

Before starting the assay, the magnetic beads and microplate were cleaned with buffer solutions. The magnetic beads (10 mg mL⁻¹) was separated from 150 µL using a magnet and redispersed in a centrifuge tube with a washing buffer. It was washed twice with 2xB&W buffer (1500 µL). The obtained magnetic beads were resuspended in 150 µL of the suitable buffer for further use. For microplate cleaning, each well on the microplate was washed with 160 µL of washing buffer twice before adding the magnetic beads. The suitable buffer used in each assay was used to clean microplate once before starting that assay.

a. Preliminary test

In this study, three different binding methods for binding cDNA on magnetic beads were studied (3 assays). For the first assay (Figure 4.3A), 112.5 µL of magnetic beads was mixed with 37.5 µL of biotinylated *C. parvum* capture probe (cDNA) in 1xB&W buffer to give a final cDNA concentration of 2.5 µmol L⁻¹ in a centrifuge tube. It was incubated in a shaker for 30 min at room temperature. After that, the obtained

magnetic beads were separated, washed with PBS buffer, and resuspend in 112.5 μL hybridization buffer. Then, 5 μL of this obtained magnetic beads was pipetted to each well and washed again with hybridization buffer. A 100 μL of tDNA (0, 5, or 100 nmol L^{-1}) and 100 μL of $\text{Ru}(\text{bpy})_3^{2+}$ -liposomes (909 $\mu\text{mol L}^{-1}$ total lipid concentration) was mixed in the well. After 30 min-incubation, the obtained beads were washed with hybridization buffer and collected for further fluorescence detection.

For second assay (Figure 4.3B), the magnetic beads were modified in the same way as performed in the first assay. For loading tDNA, 5 μL of the obtained magnetic beads was pipetted into each well and washed again with the hybridization buffer. Then, 100 μL of tDNA (0, 5, or 100 nmol L^{-1}) was pipetted into the well. After 30-min incubation, the obtained beads were washed with the hybridization buffer. After that, 100 μL of $\text{Ru}(\text{bpy})_3^{2+}$ -liposomes in HSS buffer (909 $\mu\text{mol L}^{-1}$ total lipid concentration) was added to the beads and incubated for 30 min. The beads were collected for further fluorescence detection.

For the last assay (Figure 4.3C), magnetic beads were modified with cDNA in a well plate. 5 μL of magnetic beads was mixed with 95 μL of cDNA to give the final cDNA concentration of 2.5 $\mu\text{mol L}^{-1}$. The mixture was incubated for 30 min at room temperature. After that, the procedure for loading tDNA and $\text{Ru}(\text{bpy})_3^{2+}$ -liposomes was carried out as done in the second assay. The beads were collected for further fluorescence detection.

For the detection, the beads with a bound sandwich complex from each assay were washed three times with Tris-HCl and lysed in ECL-solution for 15 min. Finally, the fluorescence signal of obtained solutions was measured.

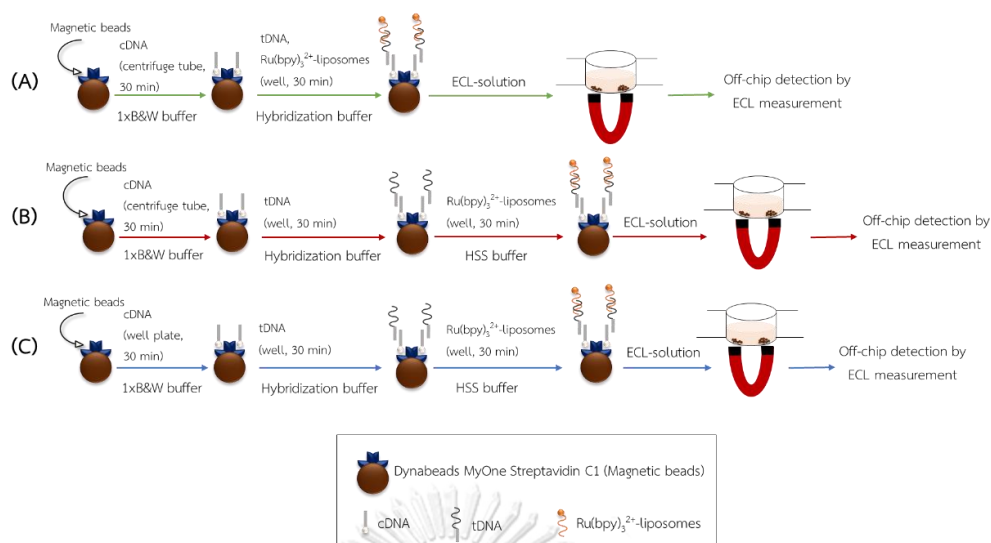


Figure 4.3 The procedure of preliminary test (A) assay A - two-step/binding cDNA in centrifuge tube, (B) assay B - three-step/binding cDNA in centrifuge tube, (C) assay C - three-step/binding cDNA in well plate.

b. The amount of $\text{Ru}(\text{bpy})_3^{2+}$ -liposomes

After the preliminary test, assay C (three-step/binding cDNA in well) in Figure 4.3C was chosen for the detection of *C. parvum* target. In this experiment, the effect of amount of $\text{Ru}(\text{bpy})_3^{2+}$ -liposomes was studied. The concentration of stock $\text{Ru}(\text{bpy})_3^{2+}$ -liposomes was presented in terms of total lipid concentration that was determined from ICP-OES. The results from ICP-OES showed the total lipid concentration of stock liposomes of $1.051 \text{ mmol L}^{-1}$. Thus, the total lipid concentration was varied as 0.105, 0.210, 0.420, and $1.051 \text{ mmol L}^{-1}$ for tDNA detection in the range of 0-100 nmol L^{-1} . After the assay, the ECL signals were compared to determine the suitable total lipid concentration for detection of *C. parvum* target.

c. The amount of magnetic beads

The next parameter is the amount of magnetic beads. In this study, the magnetic beads modified with streptavidin for binding with cDNA was used in the assay. The magnetic beads were modified with cDNA with varied mole ratio between streptavidin on magnetic beads and cDNA as 1/0.5, 1/1.0, and 1/4.0. The magnetic

beads with these ratios were used in the assay for the detection of 100 nmol L^{-1} tDNA with different amounts (50 and 100 mg of magnetic beads). After the assay, the ECL signals were compared to find the optimal mole ratio between streptavidin and cDNA for detection of *C. parvum* target.

d. The number of assay steps

From the preliminary test, the best assay was three steps including binding of cDNA on magnetic beads, loading of tDNA, and loading liposomes as a reporter probe. In this study, the steps to perform the assay were reduced. The assay was designed in one-step, two-step, and three-step by adjusting the incubation time, the type of buffer for DNA binding reaction, and addition of sucrose in the buffer. The ECL and fluorescence signals from all assays were observed and plotted against tDNA concentrations. The limit of detection was determined and used to evaluate the performance of these assays. The best assay would be further applied in the detection on a microfluidic chip (not shown in this thesis).

4.2.4 ECL measurement

In this work, the ECL signal was measured in an in-house developed macro cell adapted from the work of Mayer and co-workers [83]. In brief, a laser-induced graphene working electrode ($\approx 49 \text{ cm}^2$) was fabricated on polyimide film by a laser engraving machine. This electrode was used in the detection together with a Pt counter electrode (i.d. 0.5 mm), and an Ag/AgCl pseudo reference electrode (i.d. 2 mm). The macro cell was connected to Autolab potentiostat and ECL signals were generated by applying a potential of 1.2 V for 30 sec in a chronoamperometric mode. For detecting ECL emissions, an optical fiber (i.d. 1 cm) was used to detect the ECL emission at 610 nm with a luminescence spectrometer. The ECL intensity integrals were taken from the AB2 software.

4.2.5 Fluorescence measurement

After the assay, the obtained liposome solution was lysed by ECL-solution and analyzed for fluorescence signal by a BioTek multi-mode microplate reader. The

reader was controlled by the Gen5 Data Analysis Software and set λ_{ex} and λ_{em} as 450 and 620 nm, respectively.

4.3 Results and discussions

4.3.1 Preliminary test

The results of tDNA analysis by three different assays using different methods for cDNA binding on magnetic beads (assay A – C) are shown in the Figure 4.4. In assays A and B, when the magnetic beads were bound with cDNA in the centrifuge tube and used, the results were observed with high standard deviation when compared with the binding of cDNA in an individual well on a microplate. This might be explained by the poor dispersion of large-amount magnetic beads in the centrifuge tube that affected the binding between the biotin binding site on the magnetic beads with the biotin on cDNA required for detecting tDNA. Consequently, despite being prepared in the same centrifuge tube, the magnetic beads contained varied amounts of binding site for tDNA. Moreover, in assay A, by loading the tDNA and reporter probe to the magnetic beads in one step (Figure 4.3A), large standard deviation of the results was also observed. It was likely that some of tDNA would bind with liposome in solution, but not with cDNA on the magnetic beads. Therefore, tDNA was partially lost in the washing step. For this reason, the assay C (Figure 4.3C) was chosen for the next study.

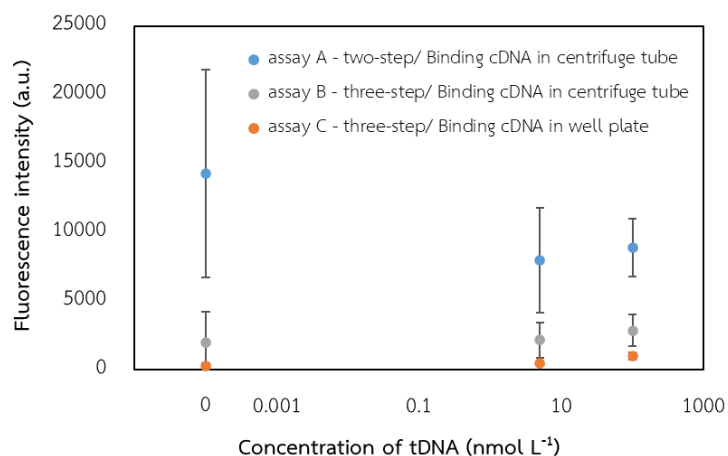


Figure 4.4 Steps in performing the assay: assay A - two-step/binding cDNA in centrifuge tube, assay B - three-step/binding cDNA in centrifuge tube, assay C - three-step/binding cDNA in well plate.

4.3.2 The amounts of liposomes

In this experiment, the amounts of liposomes were optimized by varying the total lipid concentration as 0.105, 0.210, 0.420, and 1.051 mmol L⁻¹. The results showed that an increase in lipid concentration or liposome amounts enhanced the ECL signal in the blank and in 100 mmol L⁻¹ tDNA detection as shown in Figure 4.5. However, high ECL signal in the blank could affect the detection of low concentration of tDNA due to the high background signal, and hence lower the detection sensitivity. Despite high ECL signal obtained by using 1.051 mmol L⁻¹ total lipid, it gave a high standard deviation, compared to those observed by using 0.105 mmol L⁻¹ total lipid concentration. From the results, the use of total lipid concentration at 0.105 mmol L⁻¹ was chosen because it showed the lowest ECL signal in the blank solution.

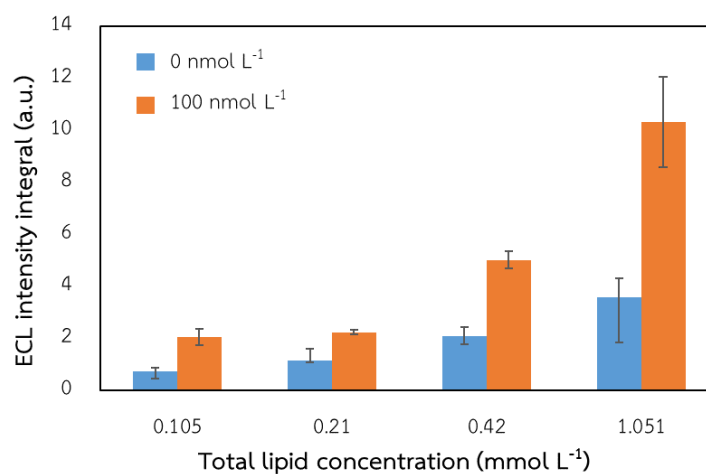


Figure 4.5 Effect of the liposomes amount in the detection of tDNA (100 nmol L⁻¹) in the three-step assay compared to blank (n=4).

4.3.3 The amount of magnetic beads

The effect of magnetic beads amount on the tDNA detection was investigated in this study. The content of cDNA for tDNA detection could be affected by the content of cDNA binding site or streptavidin on the surface of magnetic beads. Figure 4.6 presents the ECL signal observed when magnetic beads prepared by using different mole ratios of streptavidin on magnetic beads and cDNA were applied to detect tDNA. The streptavidin/mole cDNA mole ratio was varied as 1/0.5, 1/1, and 1/4. Also, the amount of these magnetic beads was varied as 50 and 100 μg in the detection of 100 nmol L⁻¹ tDNA. The results showed that using 100 μg of magnetic beads did not produce a significantly different signal from the use of 50 μg of magnetic beads. Moreover, the difference of cDNA loading on magnetic beads did not affect the assay performance. The result indicated that the use of 1/0.5 of streptavidin/cDNA mole ratio was enough for tDNA detection in this assay condition. Thus, 50 μg of magnetic beads prepared with 1/0.5 of streptavidin/cDNA mole ratio was chosen as the optimized condition.

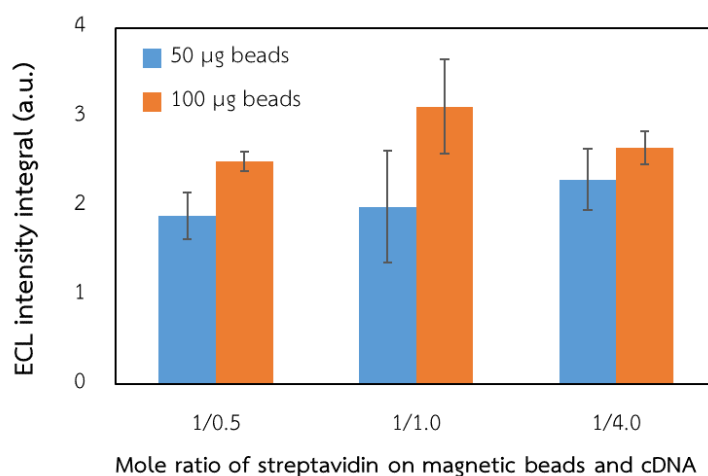


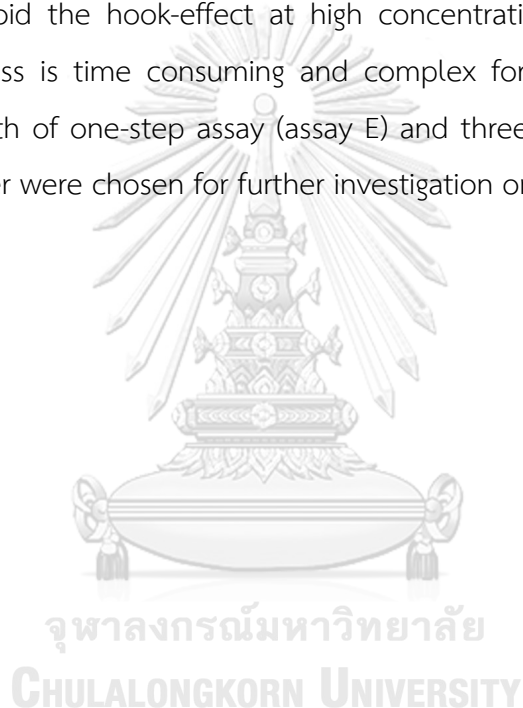
Figure 4.6 Effect of magnetic beads amount (50 and 100 µg) and the mole ratio of streptavidin on magnetic beads and cDNA on the detection of 100 nmol L⁻¹ tDNA in three-step assay (n=4).

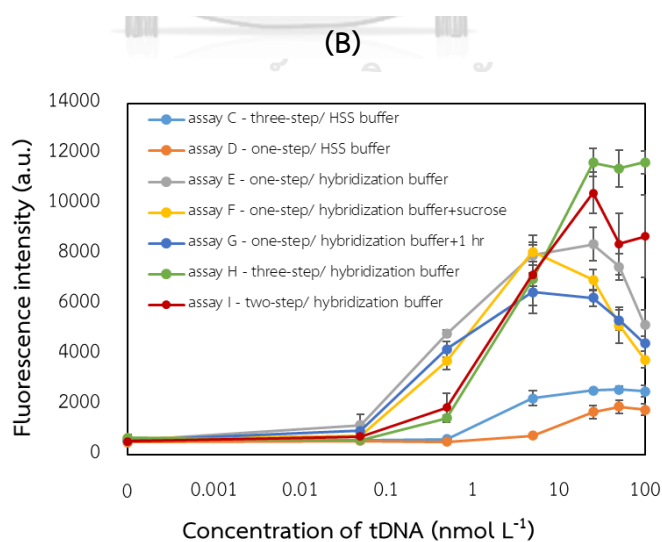
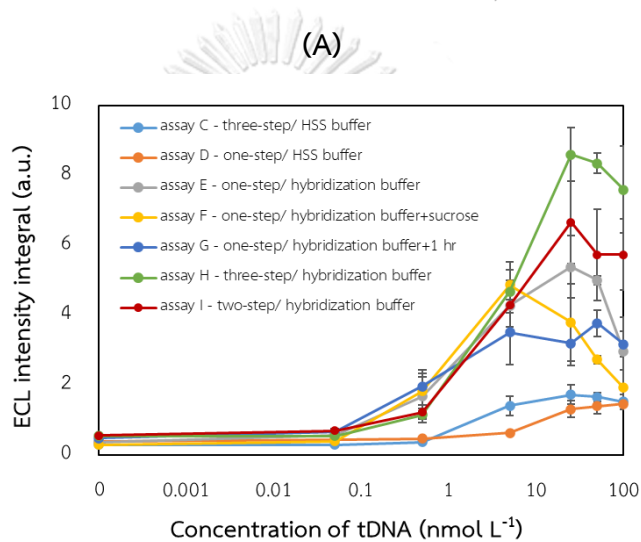
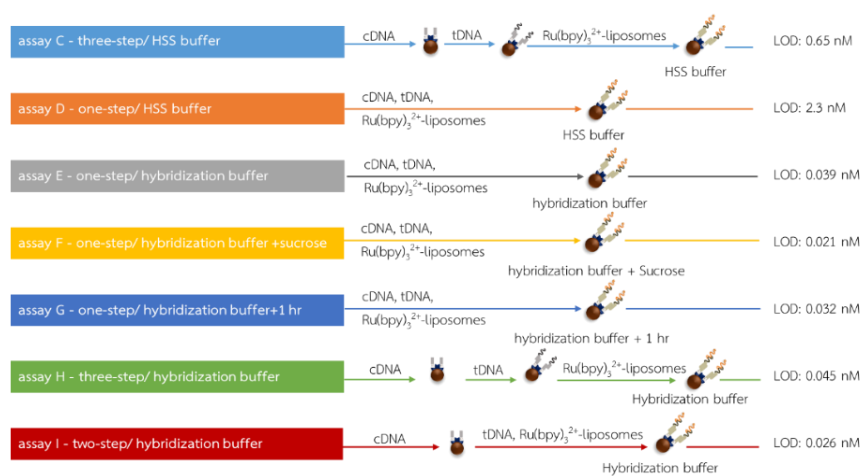
4.3.4 The number of assay steps

In this experiment, assays with different number of steps were designed to find the most suitable one with less steps (Figure 4.7A). This would be beneficial for the further application of the assay on microfluidic chips. It would decrease the complexity and analysis time. In this experiment, the magnetic beads (50 mg) prepared with a 1/0.5 streptavidin on magnetic beads/cDNA mole ratio was used to detect tDNA in the range of 0 – 100 nmol L⁻¹ with liposome with total lipid concentration of 0.105 mmol L⁻¹. The solution of all assays after lysing with ECL-solution was analyzed by ECL and fluorescence measurement.

The signals and limit of detection of all assays are shown in Figure 4.7. The one-step assay was the first choice and performed by using the HSS buffer or hybridization buffer (assay D and E). By using hybridization buffer for DNA binding reaction, higher signal could be obtained, compared to the use of HSS buffer. Therefore, the hybridization buffer was chosen for further assays. However, a decrease of signal was observed at high concentrations of tDNA because of the hook-effect [84]. The hook-effect occurred as the excess tDNA bound with cDNA in

solution instead of cDNA on the surface of magnetic beads. Hence, tDNA was partially lost, resulting in lower signal. To solve this problem, sucrose was added in the hybridization buffer (assay F) and the incubation time was prolonged to 1 hr (assay G). Unfortunately, the same phenomenon still occurred, indicating that the binding between cDNA on the magnetic beads with tDNA and between tDNA with liposomes should be done separately to obtain quantitative amount of sandwich complex on the magnetic beads. Therefore, the binding steps were performed in two steps (assay I) and three steps (assay H) instead. It was found that the three-step process could avoid the hook-effect at high concentrations of tDNA. Despite the results, this process is time consuming and complex for the application on chip. Therefore, the both of one-step assay (assay E) and three-step assay (assay H) with hybridization buffer were chosen for further investigation on microfluidic chips.





(C)

Figure 4.7 (A) the procedure for all assays, the dose-response curve obtained by (B) ECL measurement and (C) fluorescence measurement ($n=4$).

CHAPTER 5

CONCLUSION

The objectives of this dissertation were to develop methods for the detection of formaldehyde and pathogen in water samples. Two methods have been successfully developed for digital image based colorimetric detection of formaldehyde using silver-doped hydroxyapatite (Ag-HAP) and Agar-HPMC composite gel modified with Schiff's reagent (Schiff-gel). For pathogen detection, an assay for *C. parvum* DNA detection with electrochemical luminescence was designed and optimized.

For the silver-doped hydroxyapatite method, the detection was based on Tollens' reaction on Ag-HAP surface. Hydroxyapatite was synthesized via co-precipitation and its crystalline structure was characterized by X-ray diffraction spectrometer. Hydroxyapatite was modified silver ions (Ag-HAP). After reaction with formaldehyde, silver nanoparticles were produced on the surface of the Ag-HAP, resulting a material color change from off-white to yellow and brown depending on formaldehyde concentration. The effect of silver ion concentration, sodium hydroxide concentration, contact time, and sample volume was studied. Under optimized condition, hydroxyapatite was modified with 100 mg L⁻¹ silver ions solution for the detection of formaldehyde in a 5.00 mL-sample containing 0.15 mol L⁻¹ sodium hydroxide with a contact time of 30 min. The working range of formaldehyde determination was 15 – 200 µg L⁻¹ with a lowest concentration for the detection of 15 µg L⁻¹. Finally, the proposed method was successfully applied to detect formaldehyde in the drinking water, residual water from biology laboratory, and simulation runoff fishpond. The obtained results from the proposed method could be comparable with those from HPLC method, with acceptable accuracy and precision.

For the Schiff-gel method, the detection was based on the reaction of Schiff's reagent in the agar-HPMC composite gel. The Schiff-gel was prepared by mixing agar powder with HPMC and Schiff's reagent. In the presence of formaldehyde in solution,

the magenta product was produced on the surface of the Schiff-gel. The gel color changed from pale yellow to magenta depending on the concentration of formaldehyde. The effect of Schiff's reagent concentration and contact time for formaldehyde detection were examined. Under the chosen condition, Schiff-gel was prepared by using 2.50 mmol L^{-1} Schiff's reagent for the detection of formaldehyde with a contact time of 15 min. The working range of formaldehyde determination was from $2.00\text{--}10.00 \text{ mg L}^{-1}$ with the limit of detection of 1.49 mg L^{-1} . Lastly, the proposed method was successfully applied to detect formaldehyde level in water samples. The results suggested that further investigation is still required to produce analytical results with acceptable accuracy and precision.

The last project involved a development of assay for the detection of *C. parvum* DNA. The assay was developed based on the sandwich hybridization assay on the surface of magnetic beads and ECL detection. Liposome containing $\text{Ru}(\text{bpy})_3^{2+}$ was applied to enhance ELC and fluorescent signal. For assay optimization, the effect of the total lipid concentrations, mole ratio of streptavidin on magnetic beads and cDNA, and the number of steps in the assay were evaluated. Under the optimized condition, magnetic beads were prepared by using streptavidin on magnetic beads and cDNA mole ratio of 1/0.5. The ECL detection could be achieved by using liposome with the total lipid concentration of $0.105 \text{ mmol L}^{-1}$. The detection of tDNA in one-step, and three-step assay using the hybridization buffer provided high signal intensities with limit of detection of $0.039 \text{ nmol L}^{-1}$ and $0.045 \text{ nmol L}^{-1}$, respectively. The obtained assays were applied on a microfluidic platform in the future. More investigations are still required.

REFERENCES

- [1] S. Magana, S.M. Schlemmer, S.D. Leskinen, E.A. Kearns, D.V. Lim, Automated dead-end ultrafiltration for concentration and recovery of total coliform bacteria and laboratory-spiked *Escherichia coli* O157:H7 from 50-liter produce washes to enhance detection by an electrochemiluminescence immunoassay, *J Food Prot*, 76 (2013) 1152-1160.
- [2] H.O.K. Daniel R. Dietrich, *Histological analysis of endocrine disruptive effects in small laboratory fish*, John Wiley & Sons, Inc., 2009.
- [3] J.F. Leal, M.G.P.M.S. Neves, E.B.H. Santos, V.I. Esteves, Use of formalin in intensive aquaculture: properties, application and effects on fish and water quality, *Rev. Aquac*, 10 (2018) 281-295.
- [4] Z.S. Can, M. Gurol, Formaldehyde formation during ozonation of drinking Water, *Ozone Sci Eng*, 25 (2003) 41-51.
- [5] K. Kosaka, M. Asami, T. Nakai, K. Ohkubo, S. Echigo, M. Akiba, Formaldehyde formation from tertiary amine derivatives during chlorination, *Sci Total Environ*, 488-489 (2014) 325-332.
- [6] R.B. R.G. Liteplo, R. Chénier, M. E. Meek, Formaldehyde, in: WHO (Ed.), 2002.
- [7] A. Songur, O.A. Ozen, M. Sarsilmaz, The toxic effects of formaldehyde on the nervous system, *Rev Environ Contam Toxicol*, 203 (2010) 105-118.
- [8] C. Bourgeois, N. Blanc, J.C. CANNOT, C. Demesmay, Towards a Non-Biased Formaldehyde Quantification in Leather: New Derivatization Conditions before HPLC Analysis of 2,4-Dinitrophenylhydrazine Derivatives, *Molecules*, 25 (2020).
- [9] X. Xu, R. Su, X. Zhao, Z. Liu, D. Li, X. Li, H. Zhang, Z. Wang, Determination of formaldehyde in beverages using microwave-assisted derivatization and ionic liquid-based dispersive liquid-liquid microextraction followed by high-performance liquid chromatography, *Talanta*, 85 (2011) 2632-2638.
- [10] Y. Ma, C. Zhao, Y. Zhan, J. Li, Z. Zhang, G. Li, Separation and analysis of trace volatile formaldehyde in aquatic products by a MoO₃/polypyrrole intercalative sampling adsorbent with thermal desorption gas chromatography and mass spectrometry, *J Sep Sci*, 38 (2015) 1388-1393.

- [11] C. Martinez-Aquino, A.M. Costero, S. Gil, P. Gavina, Resorcinol Functionalized Gold Nanoparticles for Formaldehyde Colorimetric Detection, *J. Nanomater.*, 9 (2019).
- [12] K. Wei, L. Ma, G. Ma, C. Ji, M. Yin, A two-step responsive colorimetric probe for fast detection of formaldehyde in weakly acidic environment, *Dyes Pigm.*, 165 (2019) 294-300.
- [13] P. Gao, H. Jiang, W. Chen, Z. Cui, An intramolecular Mannich type reaction of ortho-amino aromatic azo dye and its detection effect for formaldehyde, *Dyes Pigm.*, 179 (2020).
- [14] L. Aksornneam, P. Kanatharana, P. Thavarungkul, C. Thammakhet, 5-Aminofluorescein doped polyvinyl alcohol film for the detection of formaldehyde in vegetables and seafood, *Anal. Methods.*, 8 (2016) 1249-1256.
- [15] P. Li, D. Zhang, Y. Zhang, W. Lu, W. Wang, T. Chen, Ultrafast and efficient detection of formaldehyde in aqueous solutions using chitosan-based fluorescent polymers, *ACS Sens.*, 3 (2018) 2394-2401.
- [16] J.B. Zeng, S.G. Fan, C.Y. Zhao, Q.R. Wang, T.Y. Zhou, X. Chen, Z.F. Yan, Y.P. Li, W. Xing, X.D. Wang, A colorimetric agarose gel for formaldehyde measurement based on nanotechnology involving Tollens reaction, *Chem Commun (Camb)*, 50 (2014) 8121-8123.
- [17] K. Chaiendoo, S. Sooksin, S. Kulchat, V. Promarak, T. Tuntulani, W. Ngeontae, A new formaldehyde sensor from silver nanoclusters modified Tollens' reagent, *Food Chem.*, 255 (2018) 41-48.
- [18] G.D.A. J. H. Robins, J. A. Pincock The structure of Schiff reagent aldehyde adducts and the mechanism of the Schiff reaction as determined by nuclear magnetic resonance spectroscopy, *Can. J. Chem.*, 58 (1980) 339-347.
- [19] A.F.S. Silva, I.C. Gonçalves, F.R.P. Rocha, Smartphone-based digital images as a novel approach to determine formaldehyde as a milk adulterant, *Food Control*, 125 (2021).
- [20] T. Qi, M. Xu, Y. Yao, W. Chen, M. Xu, S. Tang, W. Shen, D. Kong, X. Cai, H. Shi, H.K. Lee, Gold nanoprism/Tollens' reagent complex as plasmonic sensor in headspace single-drop microextraction for colorimetric detection of formaldehyde in food samples using smartphone readout, *Talanta*, 220 (2020) 121388.
- [21] I.M.G.d. Santos, L.S.N.S. Barbosa, C.X. Resende, G.d.A. Soares, E.A.d. Santos,

- Crystallographic aspects regarding the insertion of Ag⁺ ions into a hydroxyapatite structure, *Mater. Res.*, 18 (2015) 881-890.
- [22] L. L., Study on Enteric Vacant Capsules Based on Hydroxypropyl Methylcellulose Phthalate-55S, *Ann Materials Sci Eng* 5(2021).
- [23] G.S.L. William E. Benet, Louise Z. Yang, D. E. Peter Hughes, The mechanism of the reaction of the Tollens reagent, *J. Chem. Res.*, (2011) 675–677.
- [24] I.D. S. Fregert, B. Gruvberger, A simple method for the detection of formaldehyde, *Contact Derm.*, 10 (1984) 132-134.
- [25] Y.Y. Maruo, J. Nakamura, M. Uchiyama, M. Higuchi, K. Izumi, Development of formaldehyde sensing element using porous glass impregnated with Schiff's reagent, *Sens. Actuators B Chem.*, 129 (2008) 544-550.
- [26] W. Wongniramaikul, W. Limsakul, A. Choodum, A biodegradable colorimetric film for rapid low-cost field determination of formaldehyde contamination by digital image colorimetry, *Food Chem*, 249 (2018) 154-161.
- [27] M. Okada, T. Matsumoto, Synthesis and modification of apatite nanoparticles for use in dental and medical applications, *Japanese Dental Science Review*, 51 (2015) 85-95.
- [28] C.P.B. C. Guzman Vazquez, N. Munguia, Stoichiometric hydroxyapatite obtained by precipitation and sol gel processes, *Rev. Mex. de Fis.*, 51 (2005) 284–293.
- [29] N. Ichinose, H. Ura, Concentration dependence of the sol-gel phase behavior of agarose-water system observed by the optical bubble pressure tensiometry, *Sci Rep*, 10 (2020) 2620.
- [30] J.N. BeMiller, Carrageenans, in: *Carbohydrate Chemistry for Food Scientists*, 2019, pp. 279-291.
- [31] J.F. Walker, *Formaldehyde*, 2nd ed., Reinhold Publishing Corporation, New York, 1944.
- [32] Method 1667, Revision A: Formaldehyde, isobutyraldehyde, and furfural by derivatization followed by high performance liquid chromatography, in: EPA (Ed.), 1998.
- [33] P.M.E.a.M.E. Cassinelli, Formaldehyde: method, in, 2016, pp. 1-7.
- [34] T. Nash, The colorimetric estimation of formaldehyde by means of the Hantzsch Reaction, *Biochem J.*, 55 (1953) 416-421.

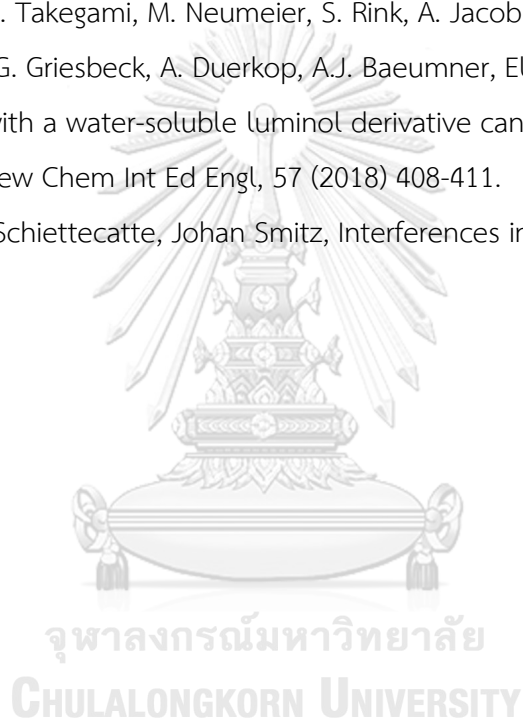
- [35] M.-S. Vesna, E. Sanja, J. Ana, V.-S. Maja, M. Miodrag, Y.C. Jung, S.J. Park, K.Y. Rhee, Electrochemical synthesis of nanosized hydroxyapatite/graphene composite powder, *Carbon letters*, 16 (2015) 233-240.
- [36] P.M. Prity Kumari, Adsorption of albumin on silica surfaces modified by silver and copper nanoparticles, *J. Nanomater.*, 2013 (2013) 1-7.
- [37] K. Lin, J. Pan, Y. Chen, R. Cheng, X. Xu, Study the adsorption of phenol from aqueous solution on hydroxyapatite nanopowders, *J Hazard Mater*, 161 (2009) 231-240.
- [38] M.T. P. Praus, M. Klementová, Preparation of silver-montmorillonite nanocomposites by reduction with formaldehyde and borohydride, *J. Braz. Chem. Soc.*, 20 (2009) 1351-1357.
- [39] H. Wang, X. Qiao, J. Chen, S. Ding, Preparation of silver nanoparticles by chemical reduction method, *Colloids Surf. A Physicochem. Eng. Asp.*, 256 (2005) 111-115.
- [40] H. Adkins, R.M. Eloffson, A.G. Rossow, C.C. Robinson, The oxidation potentials of aldehydes and ketones, *J. Am. Chem. Soc.*, 71 (1949) 3622-3629.
- [41] A. Darowska, A. Borcz, J. Nawrocki, Aldehyde contamination of mineral water stored in PET bottles, *Food Addit Contam*, 20 (2003) 1170-1177.
- [42] A. Dabrowska, J. Nawrocki, E. Szelaż-Wasielewska, Appearance of aldehydes in the surface layer of lake waters, *Environ. Monit. Assess.*, 186 (2014) 4569-4580.
- [43] Standard Format and Guidance for AOAC Standard Method Performance Requirement (SMPR) Documents, in: AOAC International, 2016.
- [44] C.F. Nascimento, M.A. Brasil, S.P. Costa, P.C. Pinto, M.L. Saraiva, F.R. Rocha, Exploitation of pulsed flows for on-line dispersive liquid-liquid microextraction: Spectrophotometric determination of formaldehyde in milk, *Talanta*, 144 (2015) 1189-1194.
- [45] S. Arsawiset, S. Teepoo, Ready-to-use, functionalized paper test strip used with a smartphone for the simultaneous on-site detection of free chlorine, hydrogen sulfide and formaldehyde in wastewater, *Anal Chim Acta*, 1118 (2020) 63-72.
- [46] A. Shahvar, M. Saraji, D. Shamsaei, Headspace single drop microextraction combined with mobile phone-based on-drop sensing for the determination of formaldehyde, *Sens. Actuators B Chem.*, 273 (2018) 1474-1478.
- [47] L. Zhang, R. Huang, W. Liu, H. Liu, X. Zhou, D. Xing, Rapid and visual detection of

- Listeria monocytogenes* based on nanoparticle cluster catalyzed signal amplification, *Biosens Bioelectron*, 86 (2016) 1-7.
- [48] H. Liu, F. Zhan, F. Liu, M. Zhu, X. Zhou, D. Xing, Visual and sensitive detection of viable pathogenic bacteria by sensing of RNA markers in gold nanoparticles based paper platform, *Biosens Bioelectron*, 62 (2014) 38-46.
- [49] Z. Fu, X. Zhou, D. Xing, Rapid colorimetric gene-sensing of food pathogenic bacteria using biomodification-free gold nanoparticle, *Sens. Actuators B Chem.*, 182 (2013) 633-641.
- [50] Z. Fu, X. Zhou, D. Xing, Sensitive colorimetric detection of *Listeria monocytogenes* based on isothermal gene amplification and unmodified gold nanoparticles, *Methods*, 64 (2013) 260-266.
- [51] L. Yao, Y. Ye, J. Teng, F. Xue, D. Pan, B. Li, W. Chen, In Vitro Isothermal Nucleic Acid Amplification Assisted Surface-Enhanced Raman Spectroscopic for Ultrasensitive Detection of *Vibrio parahaemolyticus*, *Anal Chem*, 89 (2017) 9775-9780.
- [52] D. An, Z. Chen, J. Zheng, S. Chen, L. Wang, Z. Huang, L. Weng, Determination of biogenic amines in oysters by capillary electrophoresis coupled with electrochemiluminescence, *Food Chem*, 168 (2015) 1-6.
- [53] G. Jie, J. Yuan, Novel magnetic Fe₃O₄@CdSe composite quantum dot-based electrochemiluminescence detection of thrombin by a multiple DNA cycle amplification strategy, *Anal Chem*, 84 (2012) 2811-2817.
- [54] H. Liu, X. Zhou, J. Shen, D. Xing, Sensitive Detection of Hg²⁺ with Switchable Electrochemiluminescence Luminophore and Disposable Bipolar Electrode, *ChemElectroChem*, 4 (2017) 1681-1685.
- [55] L. Li, Y. Chen, J.J. Zhu, Recent Advances in Electrochemiluminescence Analysis, *Anal Chem*, 89 (2017) 358-371.
- [56] A. Sachdeva, A.K. Singh, S.K. Sharma, An electrochemiluminescence assay for the detection of bio threat agents in selected food matrices and in the screening of *Clostridium botulinum* outbreak strains associated with type A botulism, *J Sci Food Agric*, 94 (2014) 707-712.
- [57] H. Wei, E. Wang, Electrochemiluminescence of tris(2,2'-bipyridyl)ruthenium and its applications in bioanalysis: a review, *J. Lumin.*, 26 (2011) 77-85.
- [58] K.L. Kotloff, J.P. Nataro, W.C. Blackwelder, D. Nasrin, T.H. Farag, S. Panchalingam, Y.

- Wu, S.O. Sow, D. Sur, R.F. Breiman, A.S.G. Faruque, A.K.M. Zaidi, D. Saha, P.L. Alonso, B. Tamboura, D. Sanogo, U. Onwuchekwa, B. Manna, T. Ramamurthy, S. Kanungo, J.B. Ochieng, R. Omore, J.O. Oundo, A. Hossain, S.K. Das, S. Ahmed, S. Qureshi, F. Quadri, R.A. Adegbola, M. Antonio, M.J. Hossain, A. Akinsola, I. Mandomando, T. Nhampossa, S. Acácio, K. Biswas, C.E. O'Reilly, E.D. Mintz, L.Y. Berkeley, K. Muhsen, H. Sommerfelt, R.M. Robins-Browne, M.M. Levine, Burden and aetiology of diarrhoeal disease in infants and young children in developing countries (the Global Enteric Multicenter Study, GEMS): a prospective, case-control study, *Lancet*, 382 (2013) 209-222.
- [59] C. McKerr, G.K. Adak, G. Nichols, R. Gorton, R.M. Chalmers, G. Kafatos, P. Cosford, A. Charlett, M. Reacher, K.G. Pollock, C.L. Alexander, S. Morton, An outbreak of *Cryptosporidium parvum* across England & Scotland Associated with consumption of Fresh Pre-Cut Salad Leaves, May 2012, *PLoS One*, 10 (2015) e0125955.
- [60] X. Ding, M.G. Mauk, K. Yin, K. Kadimisetty, C. Liu, Interfacing Pathogen Detection with Smartphones for Point-of-Care Applications, *Anal Chem*, 91 (2019) 655-672.
- [61] S.J. Oh, B.H. Park, G. Choi, J.H. Seo, J.H. Jung, J.S. Choi, H. Kim do, T.S. Seo, Fully automated and colorimetric foodborne pathogen detection on an integrated centrifugal microfluidic device, *Lab Chip*, 16 (2016) 1917-1926.
- [62] B.H. Park, S.J. Oh, J.H. Jung, G. Choi, J.H. Seo, D.H. Kim, E.Y. Lee, T.S. Seo, An integrated rotary microfluidic system with DNA extraction, loop-mediated isothermal amplification, and lateral flow strip based detection for point-of-care pathogen diagnostics, *Biosens Bioelectron*, 91 (2017) 334-340.
- [63] D.P. Clark, New insights into human Cryptosporidiosis, *Clin. Microbiol. Rev.*, 12 (1999) 554-563.
- [64] D.P.C. Patricia L. Meinhardt, and Kenneth B. Miller, Epidemiologic aspects of human Cryptosporidiosis and the role of waterborne transmission, *Epidemiol. Rev.*, 18 (1996) 118-136.
- [65] A.R. Jex, H.V. Smith, P.T. Monis, B.E. Campbell, R.B. Gasser, *Cryptosporidium*--biotechnological advances in the detection, diagnosis and analysis of genetic variation, *Biotechnol Adv*, 26 (2008) 304-317.
- [66] R.Y.S. Lynne S. Garcia, Evaluation of nine Immunoassay kits (Enzyme Immunoassay and Direct Fluorescence) for detection of *Giardia lamblia* and *Cryptosporidium*

- parvum in human fecal specimens, *J. Clin. Microbiol.*, 35 (1997) 1526–1529.
- [67] S.P. Johnston, M.M. Ballard, M.J. Beach, L. Causer, P.P. Wilkins, Evaluation of three commercial assays for detection of *Giardia* and *Cryptosporidium* organisms in fecal specimens, *J Clin Microbiol*, 41 (2003) 623-626.
- [68] Y. Maruyama, J.M. Feola, C. Magura, Radiosensitivity of *C. parvum*-stimulated spleen to acute ^{60}Co and low dose rate ^{137}Cs and ^{252}Cf irradiation, *Int J Radiat Biol Relat Stud Phys Chem Med*, 46 (1984) 779-785.
- [69] R. Mi, X. Yang, Y. Huang, L. Cheng, K. Lu, X. Han, Z. Chen, Immunolocation and enzyme activity analysis of *Cryptosporidium parvum* enolase, *Parasit Vectors*, 10 (2017) 273.
- [70] K.A. Edwards, A.J. Baeumner, Liposomes in analyses, *Talanta*, 68 (2006) 1421-1431.
- [71] Q. Liu, B.J. Boyd, Liposomes in biosensors, *Analyst*, 138 (2013) 391-409.
- [72] M.M. Richter, Electrochemiluminescence (ECL), *Chem. Rev.*, 104 (2004) 3003-3036.
- [73] W. Miao, Electrogenated chemiluminescence and its biorelated applications, *Chem. Rev.*, 108 (2008) 2506-2553.
- [74] S.E. Kirschbaum, A.J. Baeumner, A review of electrochemiluminescence (ECL) in and for microfluidic analytical devices, *Anal Bioanal Chem*, 407 (2015) 3911-3926.
- [75] Y. Xu, Y. Gao, T. Li, Y. Du, J. Li, E. Wang, Highly efficient electrochemiluminescence of functionalized tris(2,2'-bipyridyl)ruthenium(II) and selective concentration enrichment of its coreactants, *Adv. Funct. Mater.*, 17 (2007) 1003-1009.
- [76] G.M.G. Andrew W. Knight, Relationship between structural attributes and observed electrogenerated chemiluminescence (ECL) activity of tertiary amines as potential analytes for the tris(2,2'-bipyridine)ruthenium(II) ECL reaction. A review, *Analyst*, 121 (1996) 101R-106R.
- [77] M.K.-H. Giovanni C. Fiaccabrino, Yun-Tai Hsueh, Scott D. Collins, Rosemary L. Smith, Electrochemiluminescence of tris(2,2'-bipyridine)ruthenium in water at carbon microelectrodes, *Anal. Chem.*, 70 (1998) 4157-4161.
- [78] Y. Chen, S. Zhou, L. Li, J.-j. Zhu, Nanomaterials-based sensitive electrochemiluminescence biosensing, *Nano Today*, 12 (2017) 98-115.
- [79] S. Han, W. Niu, H. Li, L. Hu, Y. Yuan, G. Xu, Effect of hydroxyl and amino groups on electrochemiluminescence activity of tertiary amines at low tris(2,2'-bipyridyl)ruthenium(II) concentrations, *Talanta*, 81 (2010) 44-47.

- [80] K.B.B. Jari Rautio, Juhani Lahdenperä, Antje Breitenstein, Søren Molin³ and Peter Neubauer, Sandwich hybridisation assay for quantitative detection of yeast RNAs in crude cell lysates, *Microbial Cell Factories*, 2 (2003) 1-9.
- [81] K.A. Edwards, A.J. Bäumner, Optimization of DNA-tagged liposomes for use in microtiter plate analyses, *Anal Bioanal Chem*, 386 (2006) 1613-1623.
- [82] K.A. Edwards, K.L. Curtis, J.L. Sailor, A.J. Bäumner, Universal liposomes: preparation and usage for the detection of mRNA, *Anal Bioanal Chem*, 391 (2008) 1689-1702.
- [83] M. Mayer, S. Takegami, M. Neumeier, S. Rink, A. Jacobi von Wangelin, S. Schulte, M. Vollmer, A.G. Griesbeck, A. Duerkop, A.J. Bäumner, Electrochemiluminescence bioassays with a water-soluble luminol derivative can outperform fluorescence Assays, *Angew Chem Int Ed Engl*, 57 (2018) 408-411.
- [84] E.A. Johan Schiettecatte, Johan Smitz, Interferences in immunoassays, *InTech*, 2012.





จุฬาลงกรณ์มหาวิทยาลัย
CHULALONGKORN UNIVERSITY

VITA

NAME Uma Pongkitdachoti

DATE OF BIRTH 28 February 1990

PLACE OF BIRTH Bangkok, Thailand

INSTITUTIONS ATTENDED M. SC., Chemistry, Chulalongkorn University, Bangkok, Thailand, August 2015
B. SC., Chemistry, Chulalongkorn University, Bangkok, Thailand, April 2012

PUBLICATION

1. Pongkitdachoti, U.; Unob, F. Simultaneous adsorption of silver nanoparticles and silver ions on large pore mesoporous silica. *Journal of Environmental Chemical Engineering*. 2018, 6, 596-603.
2. Pongkitdachoti, U.; Unob, F. Silver-doped hydroxyapatite for formaldehyde determination by digital-image colorimetry. *Analytical Methods*. 2022, 14, 926-934.